



A robust SUPG norm a posteriori error estimator for stationary convection–diffusion equations



Volker John^{a,b,*}, Julia Novo^{c,1}

^aWeierstrass Institute for Applied Analysis and Stochastics, Leibniz Institute in Forschungsverbund Berlin e.V. (WIAS), Mohrenstr. 39, 10117 Berlin, Germany

^bFree University of Berlin, Department of Mathematics and Computer Science, Arnimallee 6, 14195 Berlin, Germany

^cDepartamento de Matemáticas, Universidad Autónoma de Madrid, Madrid, Spain

ARTICLE INFO

Article history:

Received 23 May 2012

Received in revised form 21 November 2012

Accepted 23 November 2012

Available online 14 December 2012

Keywords:

Stationary convection–diffusion equations

SUPG finite element method

Error in SUPG norm

A posteriori error estimator

Adaptive grid refinement

ABSTRACT

A robust residual-based a posteriori estimator is proposed for the SUPG finite element method applied to stationary convection–diffusion–reaction equations. The error in the natural SUPG norm is estimated. The main concern of this paper is the consideration of the convection-dominated regime. A global upper bound and a local lower bound for the error are derived, where the global upper estimate relies on some hypotheses. Numerical studies demonstrate the robustness of the estimator and the fulfillment of the hypotheses. A comparison to other residual-based estimators with respect to the adaptive grid refinement is also provided.

© 2012 Elsevier B.V. All rights reserved.

1. Introduction

A posteriori error estimation in the context of stationary convection-dominated convection–diffusion–reaction equations is studied in this paper. This kind of equations describe the transport of a quantity such as temperature or concentration. In applications, the convective forces usually dominate the diffusive forces. In this case, standard discretization methods do not provide good approximations. Stabilization techniques are employed to produce accurate numerical approximations. The study of appropriate schemes to deal with the convection-dominated regime is a subject that has received a lot of attention in the last decades, see [21,23] for an overview of methods and of results. The most popular stabilized finite element method is the Streamline-Upwind Petrov–Galerkin (SUPG) method introduced in [3,12]. This method will be considered in the present paper. The numerical results obtained with the SUPG method are generally not perfect because there are often spurious oscillations in a vicinity of layers. Nevertheless, the SUPG method has been proved in a competitive study of stabilized discretizations [2] as a good choice to compute approximations where sharpness and position of layers are impor-

tant. With respect to efficiency (quality of the computed solution per computing time), this method outperformed all modern approaches that were included in the studies of [2].

In the review [23], the author prognosticates that adaptive methods will triumph over all types of convection–diffusion problems, although much work remains to be done. It is well known that for the design of an adaptive method the provision of an appropriate a posteriori error estimator is necessary. A robust (with respect to the ratio of diffusion and convection) upper estimate serves as actual error estimate and stopping criterion of the solution process. Local lower estimates control an adaptive grid refinement. About a decade ago, a competitive study of a number of proposed error estimators for the SUPG solution of convection-dominated convection–diffusion equations [16] came to the conclusion that none of them is robust and that the quality of the adaptively refined grids is often not satisfactory. Since then, only a few contributions concerning new a posteriori error estimators for the considered class of problem and type of discretization can be found in the literature. The important ones [26,22,9,10] will be discussed below.

In the present paper, robust residual-based a posteriori error bounds are derived for the error of the SUPG finite element approximation. The error bounds are obtained in the norm typically used in the a priori analysis of this method. Since the SUPG method is the most popular stabilized finite element method for convection–diffusion problems, there were of course attempts to derive a posteriori error estimates for this method. In Verfürth [25], an

* Corresponding author at: Weierstrass Institute for Applied Analysis and Stochastics, Leibniz Institute in Forschungsverbund Berlin e.V. (WIAS), Mohrenstr. 39, 10117 Berlin, Germany.

E-mail addresses: john@wias-berlin.de (V. John), julia.novo@uam.es (J. Novo).

¹ The research was supported by Spanish MEC under Grant MTM2010-14919.

a posteriori error bound is presented for the error in the norm $(\varepsilon \|\nabla v\|_0^2 + \|v\|_0^2)^{1/2}$, ε being the diffusion parameter. This bound is not robust. An extension of the analysis of [25] led in [26] to a robust error estimator for a norm that adds to the norm of [25] a dual norm of the convective derivative. The additional term in this norm can be only approximated. Some error bounds are also proved in [22] in the one-dimensional case in a norm that includes a semi-norm of the error of order 1/2. Robust a posteriori error estimators for the $L^1(\Omega)$ and $L^2(\Omega)$ norm of the error can be found in [8–10]. Unlike the approaches from, e.g., [25,26] and the approach used in the present paper, the derivation of these estimators is based on the variational multiscale theory [14]. It can be applied to stabilized discretizations since their error distribution is practically local [13]. The essential part in the derivation consists in computing or approximating an appropriate norm of a local Green's function, see [10] for the P_1 and Q_1 finite element in two dimensional situations, and [9] for higher order finite elements in one dimension. However, the $L^1(\Omega)$ and $L^2(\Omega)$ norm are comparably weak norms, e.g., spurious oscillations of the numerical solution contribute generally little to the errors in these norms. The a priori error analysis is performed usually for stronger norms, like the SUPG norm for the SUPG discretization. In Hauke et al. [9], a remark can be found concerning the extension of the approach based on the variational multiscale theory to the $H^1(\Omega)$ semi norm, but we are not aware of the derivation of concrete estimators. In summary, there are robust a posteriori error estimates in the literature but only for norms that do not show up in the a priori analysis or that are hard to compute or that are, in our opinion, not of interest in applications.

The main goal of this paper is to prove a robust a posteriori error bound for the method in the same norm as it is used in the a priori error analysis, namely the SUPG norm. As shall be seen in Section 3, the derivation of the upper bound will use some hypotheses. These hypotheses are probably not fulfilled in the worst case. But it will be argued and checked numerically that they are true in standard situations. Because of the hypotheses, the obtained results are from the mathematical point of view less general than, e.g., the results of [26]. However, we think that from the practical point of view the derivation of a robust error estimator for the natural norm of the SUPG method is of interest. A similar situation can be found in [4], where the derivation of an a posteriori error estimator for the natural norm of some other stabilized discretization is also based on an assumption (a saturation assumption) that most probably is not satisfied in the worst case.

The paper is organized as follows. In Section 2, the considered equations, some preliminaries, and notations are presented. Section 3 is devoted to the derivation of a robust global upper bound for the error in the SUPG norm. Hypotheses that relate the error of an interpolant in different norms and the error of the SUPG approximation will be assumed. A comparison between the derived error estimator and other residual-based error estimators from the literature is provided in Remark 4. In Section 4, local lower bounds for the error are obtained. Both in Sections 3 and 4, the convection-dominated regime is considered to be able to bound the errors in the SUPG norm. The key point is that in this regime there are two additional terms in the bounds that are negligible in this case compared with the other terms, see Remarks 3 and 6. On the other hand, in the diffusion-dominated regime, the derived error estimator possesses the same weights as the estimators from [25,26], see Remark 4. Section 5 provides numerical studies. For the derived error estimator, the robustness of the effectivity index can be observed for different examples and finite elements of different polynomial degree. With respect to the adaptive grid refinement, it turns out that the proposed error estimator tends to refine subregions with strong singularities deeper and to start the refinement of subregions with weaker singularities later than other residual-based a posteriori error estimators.

2. The equations, notations, preliminaries

Throughout the paper, standard notations are used for Sobolev spaces and corresponding norms, see, e.g. [5]. In particular, given a measurable set $\omega \subset \mathbb{R}^d$, the inner product in $L^2(\omega)$ or $L^2(\omega)^d$ is denoted by $(\cdot, \cdot)_\omega$ and the notation (\cdot, \cdot) is used instead of $(\cdot, \cdot)_\Omega$. The norm (semi norm) in $W^{m,p}(\omega)$ will be denoted by $\|\cdot\|_{m,p,\omega}$ ($|\cdot|_{m,p,\omega}$), with the convention $\|\cdot\|_{m,\omega} = \|\cdot\|_{m,2,\omega}$.

This paper considers stationary convection–diffusion–reaction equations of the form

$$\begin{aligned} -\varepsilon \Delta u + \mathbf{b} \cdot \nabla u + cu &= f \quad \text{in } \Omega, \\ u &= 0 \quad \text{on } \Gamma_D, \\ \varepsilon \frac{\partial u}{\partial \mathbf{n}} &= \varepsilon \partial_{\mathbf{n}} u = g \quad \text{on } \Gamma_N, \end{aligned} \tag{1}$$

where Ω is a polygonal domain in \mathbb{R}^d , $d \geq 2$, with Lipschitz boundary Γ consisting of two disjoint components Γ_D and Γ_N . The Dirichlet part Γ_D has a positive $(d-1)$ -dimensional Lebesgue measure and $\partial\Omega^- \subset \Gamma_D$, $\partial\Omega^-$ being the inflow boundary of Ω , i.e., the set of points $\mathbf{x} \in \partial\Omega$ such that $\mathbf{b}(\mathbf{x}) \cdot \mathbf{n}(\mathbf{x}) < 0$. It will be assumed that $0 < \varepsilon$, $\mathbf{b} \in W^{1,\infty}(\Omega)$, $c \in L^\infty(\Omega)$, $f \in L^2(\Omega)$, and (1) is scaled such that $\|\mathbf{b}\|_{L^\infty(\Omega)} = \mathcal{O}(1)$, $\|c\|_{L^\infty(\Omega)} = \mathcal{O}(1)$, and $0 < \varepsilon \ll 1$. Hence, the convection-dominated regime is studied. Furthermore, it will be assumed that one of the following conditions is fulfilled: either

$$c(\mathbf{x}) - \frac{1}{2} \operatorname{div}(\mathbf{b}(\mathbf{x})) = \mu(\mathbf{x}) \geq \mu_0 > 0 \quad \forall \mathbf{x} \in \Omega, \tag{2}$$

or

$$-\frac{1}{2} \operatorname{div}(\mathbf{b}(\mathbf{x})) = \mu(\mathbf{x}) \geq \mu_0 = 0 \quad \forall \mathbf{x} \in \Omega, \quad \text{and} \quad c \equiv 0. \tag{3}$$

Then, it is well known that (1) possesses a unique weak solution $u \in H_D^1(\Omega) = \{v \in H^1(\Omega) : v|_{\Gamma_D} = 0\}$ that satisfies

$$\varepsilon(\nabla u, \nabla v) + (\mathbf{b} \cdot \nabla u, v) + (cu, v) = (f, v) + (g, v)_{\Gamma_N} \quad \forall v \in H_D^1(\Omega), \tag{4}$$

e.g. see [21].

Let $\{\mathcal{T}_h\}$, $h > 0$, be a family of partitions of Ω . In the analysis, it will be assumed that all partitions are admissible, i.e. any two (compact) mesh cells are either disjoint or they share a complete k face, $0 \leq k \leq d-1$. Furthermore, the family should be regular, i.e., there exists a constant σ such that for each mesh cell $K \in \mathcal{T}_h$ it holds $h_K/\rho_K \leq \sigma$, where h_K and ρ_K denote the diameter of K and the diameter of the largest ball inscribed into K , respectively. The characteristic parameter of the triangulation is given by $h = \max_{K \in \mathcal{T}_h} h_K$. The conforming finite element space on a triangulation \mathcal{T}_h consisting of piecewise polynomials of local degree less than or equal to r that vanish on the Dirichlet boundary will be denoted by $V_{h,r} \subset H_D^r(\Omega)$.

Since the triangulations are assumed to be regular, the following inverse inequality holds for each $v_h \in V_{h,r}$ and each mesh cell $K \in \mathcal{T}_h$, see, e.g. [5, Theorem 3.2.6],

$$\|v_h\|_{m,q,K} \leq c_{\text{inv}} h_K^{l-m-d\left(\frac{1}{q}-\frac{1}{q'}\right)} \|v_h\|_{l,q',K}, \tag{5}$$

where $0 \leq l \leq m \leq 1$ and $1 \leq q' \leq q \leq \infty$. In addition, it is assumed that the space $V_{h,r}$ satisfies the following local approximation property: for each $v \in H_D^1(\Omega) \cap H^{r+1}(\Omega)$ there exists $\hat{v}_h \in V_{h,r}$ such that

$$\|v - \hat{v}_h\|_{0,K} + h_K \|\nabla(v - \hat{v}_h)\|_{0,K} + h_K^2 \|\Delta(v - \hat{v}_h)\|_{0,K} \leq Ch_K^{r+1} \|v\|_{r+1,K}.$$

Following the notation of [25], the set of all $d-1$ faces in \mathcal{T}_h is denoted by \mathcal{E}_h . This set can be decomposed into $\mathcal{E}_h = \mathcal{E}_{h,\Omega} \cup \mathcal{E}_{h,N} \cup \mathcal{E}_{h,D}$, where $\mathcal{E}_{h,\Omega}$, $\mathcal{E}_{h,N}$ and $\mathcal{E}_{h,D}$ refer to interior faces, faces on the Neumann boundary Γ_N , and faces on the Dirichlet boundary Γ_D , respectively. For $E \in \mathcal{E}_h$, let h_E be the diameter of E . The shape

regularity of the triangulations implies that $h_K \simeq h_E$ whenever $E \subset \partial K$ and $h_K \simeq h_{K'}$ if $K \cap K' \neq \emptyset$. The set of mesh cells having a common $d - 1$ face is denoted by $\omega_E = \cup_{E \subset \partial K'} K'$. For any piecewise continuous function v and any $E \in \mathcal{E}_{h,\Omega}$, the jump of v across E in an arbitrary but fixed direction \mathbf{n}_E orthogonal to E is denoted by $[[v]]_E$. Let ω_K denote the patch of mesh cells that have a joint face with K .

Let $q \in [1, \infty)$ and let $s \in \{0, 1\}$ with $s \leq t \leq r + 1$. Then, I_h denotes a bounded linear interpolation operator $I_h : W^{t,q}(\Omega) \rightarrow V_{h,r}$ that satisfies for all $v \in W^{t,q}(\Omega)$ and all mesh cells $K \in \mathcal{T}_h$

$$|v - I_h v|_{s,q,K} \leq Ch_K^{t-s} |v|_{t,q,K}, \tag{6}$$

e.g. see [5]. Using the technique of [20, Lemma 2.1], one obtains for all $v \in H^1_D(\Omega) \cap H^{r+1}(\Omega)$ the estimate

$$\|\Delta(v - I_h v)\|_{0,K}^2 \leq Ch_K^{2r-2} \|v\|_{r+1,K}^2 \quad \forall K \in \mathcal{T}_h. \tag{7}$$

A local trace inequality that takes the size of the mesh cell into account was proved in [25, Lemma 3.1]: For $v \in H^1(K)$ and $E \subset \partial K$ it holds

$$\|v\|_{0,E} \leq C \left(h_E^{-1/2} \|v\|_{0,K} + \|v\|_{0,K}^{1/2} \|\nabla v\|_{0,K}^{1/2} \right). \tag{8}$$

For presenting the SUPG finite element discretization of (1), the bilinear form $a_{\text{SUPG}}(\cdot, \cdot) : H^1_D \times H^1_D \rightarrow \mathbb{R}$ is introduced

$$a_{\text{SUPG}}(u, v) = \varepsilon(\nabla u, \nabla v) + (\mathbf{b} \cdot \nabla u, v) + (cu, v) + \sum_{K \in \mathcal{T}_h} \delta_K (-\varepsilon \Delta u + \mathbf{b} \cdot \nabla u + cu, \mathbf{b} \cdot \nabla v)_K,$$

where δ_K is the stabilization parameter (generally a function depending on \mathbf{x}). There are several proposals for concrete choices of δ_K available in the literature, see [17] for an overview. All proposals possess the same asymptotic limits $\delta_K = \mathcal{O}(h_K / \|\mathbf{b}\|_{K,\infty})$ in the convection-dominated regime $Pe_K \gg 1$ and $\delta_K = \mathcal{O}(h_K^2 / \varepsilon)$ in the diffusion-dominated regime $Pe_K \leq 1$, where

$$Pe_K = \frac{\|\mathbf{b}\|_{\infty,K} h_K}{2r\varepsilon}$$

is the local Péclet number. Only these limits are important for a discussion of the analytical results. To facilitate this discussion, the following concrete proposal from [23, (10.11)] is considered

$$\delta_K = \begin{cases} \delta_0 \frac{h_K}{\|\mathbf{b}\|_{\infty,K}} & \text{if } Pe_K \geq 1, \\ \delta_1 \frac{h_K^2}{\varepsilon} & \text{else,} \end{cases} \tag{9}$$

where δ_0 and δ_1 are user-chosen constants. In the convection-dominated regime, the particular value $\delta_0 = (2 \max\{r, C_K^2\})^{-1}$ will be chosen, where C_K is a constant defined below in (43) and (44). Then, the SUPG finite element method reads as follows: Find $u_h \in V_{h,r}$ such that

$$a_{\text{SUPG}}(u_h, v_h) = (f, v_h) + (g, v_h)_{\Gamma_N} + \sum_{K \in \mathcal{T}_h} \delta_K (f, \mathbf{b} \cdot \nabla v_h)_K \quad \forall v_h \in V_{h,r}. \tag{10}$$

The natural norm for performing the a priori error analysis of (10) is given by

$$\|v\|_{\text{SUPG}} := \left(\varepsilon \|\nabla v\|_0^2 + \sum_{K \in \mathcal{T}_h} \delta_K \|\mathbf{b} \cdot \nabla v\|_{0,K}^2 + \|\mu^{1/2} v\|_0^2 \right)^{1/2} \tag{11}$$

in the case $\mu_0 > 0$ and by

$$\|v\|_{\text{SUPG}} := \left(\varepsilon \|\nabla v\|_0^2 + \sum_{K \in \mathcal{T}_h} \delta_K \|\mathbf{b} \cdot \nabla v\|_{0,K}^2 \right)^{1/2} \tag{12}$$

in the case $\mu_0 = 0$. A straightforward calculation shows that the SUPG method satisfies the Galerkin orthogonality

$$a_{\text{SUPG}}(u - u_h, v_h) = 0, \quad \forall v_h \in V_{h,r}. \tag{13}$$

3. A global upper error bound

This section provides the global upper a posteriori bound of the error. The analysis concentrates on the convection-dominated case and it relies on Hypothesis 1 below that relates interpolation errors in different norms and the error of the SUPG approximation in the SUPG norm. Hypothesis 1 will be discussed in detail and numerically checked in Section 5. The diffusion-dominated regime will be discussed in Remark 4.

Hypothesis 1. It will be assumed that several norms of the interpolation error $u - I_h u$ can be bounded by norms of the error $u - u_h$:

$$\sum_{K \in \mathcal{T}_h} \delta_K^{-1} \|u - I_h u\|_{0,K}^2 \leq 2 \|u - u_h\|_{\text{SUPG}}^2, \tag{14}$$

$$\sum_{K \in \mathcal{T}_h} \delta_K \|\mathbf{b} \cdot \nabla(u - I_h u)\|_{0,K}^2 \leq 2 \|u - u_h\|_{\text{SUPG}}^2, \tag{15}$$

$$\sum_{E \in \mathcal{E}_h} \|\mathbf{b}\|_{\infty,E} \|u - I_h u\|_{0,E}^2 \leq 2 \|u - u_h\|_{\text{SUPG}}^2. \tag{16}$$

Remark 1 (Discussion of Hypothesis 1). Hypothesis 1 is only needed in the convection-dominated case. Let $u \in H^1_D(\Omega) \cap H^{r+1}(\Omega)$ and consider a family of uniform triangulations. Since $r \geq 1$ it follows that $u \in H^2(\Omega)$ and then the Lagrange interpolation operator can be used. From the error analysis of the SUPG method, it is well known [21] that the estimate

$$\|u - u_h\|_{\text{SUPG}}^2 = \mathcal{O}(h^{2r+1}) \tag{17}$$

holds. Using the optimal choice $\delta_K = \mathcal{O}(h_K)$ of the stabilization parameter, as given e.g. by (9), one gets from the interpolation estimate (6)

$$\sum_{K \in \mathcal{T}_h} \delta_K^{-1} \|u - I_h u\|_{0,K}^2 = \mathcal{O}(h^{2r+1}),$$

$$\sum_{K \in \mathcal{T}_h} \delta_K \|\mathbf{b} \cdot \nabla(u - I_h u)\|_{0,K}^2 \leq \|\mathbf{b}\|_{\infty}^2 \sum_{K \in \mathcal{T}_h} \delta_K \|\nabla(u - I_h u)\|_{0,K}^2 = \mathcal{O}(h^{2r+1}).$$

With the trace estimate (8), one obtains also

$$\sum_{E \in \mathcal{E}_h} \|\mathbf{b}\|_{\infty,E} \|u - I_h u\|_{0,E}^2 \leq C \sum_{K \in \mathcal{T}_h} \left(h_K^{-1} \|u - I_h u\|_{0,K}^2 + \|u - I_h u\|_{0,K} \|\nabla(u - I_h u)\|_{0,K} \right) = \mathcal{O}(h^{2r+1}).$$

Hence, all terms in (14)–(16) are of the same order with respect to h .

It is well known from numerical simulations that the solutions obtained with the SUPG method are polluted with spurious oscillations in a vicinity of layers [17,2]. In contrast, the interpolation $I_h u$ with the Lagrange interpolation operator is nodally exact. The absence of spurious oscillations in the interpolant justifies, in our opinion, Hypothesis 1, at least in some standard case. This statement will be supported numerically in Section 5, see particularly Example 2. Of course, we are aware that Hypothesis 1 most probably does not hold in the worst case scenario.

Lemma 1. Let $v = u - u_h$, $u \in H^2(\Omega)$ being the solution of (4) and u_h its SUPG approximation computed by solving (10). If the SUPG parameters are chosen such that

$$\delta_K \leq \frac{h_K^2}{8c_{\text{inv}}^2 \varepsilon}, \tag{18}$$

and in the case (2) also such that

$$\delta_K \leq \frac{\mu_0}{2\|c\|_{K,\infty}^2} c_{\text{inv}}^2 \tag{19}$$

then

$$a_{\text{SUPG}}(v, v) \geq \frac{1}{2} \|v\|_{\text{SUPG}}^2 - \sum_{K \in \mathcal{T}_h} 4\delta_K h_K^{-2} \varepsilon^2 c_{\text{inv}}^2 \|\nabla(u - I_h u)\|_{0,K}^2 - \sum_{K \in \mathcal{T}_h} 2\delta_K \varepsilon^2 \|\Delta(u - I_h u)\|_{0,K}^2. \tag{20}$$

Proof. The proof will be presented for the case (2). The simplifications for the case (3) are obvious. A straightforward calculation leads from the definition of $a_{\text{SUPG}}(\cdot, \cdot)$ to

$$a_{\text{SUPG}}(v, v) = \|v\|_{\text{SUPG}}^2 + \sum_{K \in \mathcal{T}_h} \delta_K (c v, \mathbf{b} \cdot \nabla v)_K - \sum_{K \in \mathcal{T}_h} \delta_K \varepsilon (\Delta v, \mathbf{b} \cdot \nabla v)_K. \tag{21}$$

The terms on the right hand side of (21) have to be bounded. Using the Cauchy–Schwarz inequality, Young’s inequality, and (19) gives directly

$$\begin{aligned} \left| \sum_{K \in \mathcal{T}_h} \delta_K (c v, \mathbf{b} \cdot \nabla v)_K \right| &\leq \sum_{K \in \mathcal{T}_h} \delta_K (c v, c v)_K + \frac{1}{4} \sum_{K \in \mathcal{T}_h} \delta_K \|\mathbf{b} \cdot \nabla v\|_{0,K}^2 \\ &\leq \sum_{K \in \mathcal{T}_h} \delta_K \frac{\|c\|_{K,\infty}^2}{\mu_0} \|\mu^{1/2} v\|_0^2 + \frac{1}{4} \sum_{K \in \mathcal{T}_h} \delta_K \|\mathbf{b} \cdot \nabla v\|_{0,K}^2 \\ &\leq \frac{1}{2} \|\mu^{1/2} v\|_0^2 + \frac{1}{4} \sum_{K \in \mathcal{T}_h} \delta_K \|\mathbf{b} \cdot \nabla v\|_{0,K}^2. \end{aligned} \tag{22}$$

The estimate of the second term on the right hand side of (21) starts also with the Cauchy–Schwarz inequality and Young’s inequality

$$\left| - \sum_{K \in \mathcal{T}_h} \delta_K \varepsilon (\Delta v, \mathbf{b} \cdot \nabla v)_K \right| \leq \sum_{K \in \mathcal{T}_h} \delta_K \varepsilon^2 \|\Delta v\|_{0,K}^2 + \frac{1}{4} \sum_{K \in \mathcal{T}_h} \delta_K \|\mathbf{b} \cdot \nabla v\|_{0,K}^2. \tag{23}$$

For the first term on the right hand side of (23), adding and subtracting $I_h u$ yields

$$\sum_{K \in \mathcal{T}_h} \delta_K \varepsilon^2 \|\Delta v\|_{0,K}^2 \leq 2 \sum_{K \in \mathcal{T}_h} \delta_K \varepsilon^2 \left(\|\Delta(u - I_h u)\|_{0,K}^2 + \|\Delta(I_h u - u_h)\|_{0,K}^2 \right). \tag{24}$$

One gets for the second term on the right hand side of (24) by applying the inverse estimate (5), adding and subtracting u , and applying the upper bound of the stabilization parameters (18)

$$\begin{aligned} \sum_{K \in \mathcal{T}_h} 2\delta_K \varepsilon^2 \|\Delta(I_h u - u_h)\|_{0,K}^2 &\leq \sum_{K \in \mathcal{T}_h} 2\delta_K \varepsilon^2 h_K^{-2} c_{\text{inv}}^2 \|\nabla(I_h u - u_h)\|_{0,K}^2 \\ &\leq 4 \sum_{K \in \mathcal{T}_h} \delta_K \varepsilon^2 h_K^{-2} c_{\text{inv}}^2 \left(\|\nabla v\|_{0,K}^2 + \|\nabla(u - I_h u)\|_{0,K}^2 \right) \\ &\leq \frac{1}{2} \varepsilon \|\nabla v\|_0^2 + 4 \sum_{K \in \mathcal{T}_h} \delta_K \varepsilon^2 h_K^{-2} c_{\text{inv}}^2 \|\nabla(u - I_h u)\|_{0,K}^2. \end{aligned} \tag{25}$$

Inserting (25) into (24), then (24) into (23) and finally (23) and (22) into (21) gives (20). \square

Remark 2 (On Lemma 1). If $\|c\|_{K,\infty} = 0$ in (19), then δ_K should be just bounded on K .

Condition (18) is fulfilled in the convection-dominated case $Pe_K \gg 1$ since

$$\delta_K = \frac{\delta_0}{2p} Pe_K^{-1} \frac{h_K^2}{\varepsilon}.$$

In the diffusion-dominated case one has to choose $\delta_1 \leq 1/(8c_{\text{inv}}^2)$. With the definition (9) of the stabilization parameter, condition (18) might be violated in some transition region between the convection- and diffusion-dominated case. However, for this region and also in the diffusion-dominated case, a different kind of analysis can be applied, see Remark 4.

The $H^2(\Omega)$ regularity of u is needed in the proof only locally, for each $K \in \mathcal{T}_h$. However, the analysis should be valid for all meshes such that the regularity assumption from Lemma 1 is appropriate. This assumption can be relaxed, e.g., in the case that $u \notin H^2(\Omega)$ but a non-smooth behavior of u occurs only on a known piecewise linear $(d - 1)$ -dimensional manifold and one considers only meshes where this manifold does not cut the interior of any mesh cell.

In the next step, a representation of the error will be derived. Using the Galerkin orthogonality (13), the weak form of Eq. (4), and integration by parts gives for all $v \in H_D^1(\Omega)$

$$\begin{aligned} a_{\text{SUPG}}(u - u_h, v) &= (f, v - I_h v) + (g, v - I_h v)_{\Gamma_N} \\ &\quad + \sum_{K \in \mathcal{T}_h} \delta_K (f, \mathbf{b} \cdot \nabla(v - I_h v))_K - \varepsilon (\nabla u_h, \nabla(v - I_h v)) \\ &\quad - (\mathbf{b} \cdot \nabla u_h, v - I_h v) - (c u_h, (v - I_h v)) \\ &\quad - \sum_{K \in \mathcal{T}_h} \delta_K (-\varepsilon \Delta u_h + \mathbf{b} \cdot \nabla u_h + c u_h, \mathbf{b} \cdot \nabla(v - I_h v))_K \\ &= \sum_{K \in \mathcal{T}_h} (f + \varepsilon \Delta u_h - \mathbf{b} \cdot \nabla u_h - c u_h, v - I_h v)_K \\ &\quad + \sum_{K \in \mathcal{T}_h} \delta_K (f + \varepsilon \Delta u_h - \mathbf{b} \cdot \nabla u_h - c u_h, \mathbf{b} \cdot \nabla(v - I_h v))_K \\ &\quad + \sum_{E \in \mathcal{E}_{h,\Omega}} (-\varepsilon \llbracket \partial_{n_E} u_h \rrbracket_E, v - I_h v)_E + \sum_{E \in \mathcal{E}_{h,N}} (g - \varepsilon \partial_{n_E} u_h, v - I_h v)_E \\ &= \sum_{K \in \mathcal{T}_h} (R_K(u_h), v - I_h v)_K + \sum_{K \in \mathcal{T}_h} \delta_K (R_K(u_h), \mathbf{b} \cdot \nabla(v - I_h v))_K \\ &\quad + \sum_{E \in \mathcal{E}_h} (R_E(u_h), v - I_h v)_E, \end{aligned} \tag{26}$$

where the mesh cell and the face residuals are defined by

$$R_K(u_h) := f + \varepsilon \Delta u_h - \mathbf{b} \cdot \nabla u_h - c u_h|_K,$$

$$R_E(u_h) := \begin{cases} -\varepsilon \llbracket \partial_{n_E} u_h \rrbracket_E & \text{if } E \in \mathcal{E}_{h,\Omega}, \\ g - \varepsilon \partial_{n_E} u_h & \text{if } E \in \mathcal{E}_{h,N}, \\ 0 & \text{if } E \in \mathcal{E}_{h,D}. \end{cases}$$

Setting $v = u - u_h$ and observing that $v - I_h v = (u - u_h) - I_h(u - u_h) = u - I_h u$ leads together with (20) to

$$\begin{aligned} \frac{1}{2} \|u - u_h\|_{\text{SUPG}}^2 &\leq \sum_{K \in \mathcal{T}_h} (R_K(u_h), u - I_h u)_K \\ &\quad + \sum_{K \in \mathcal{T}_h} \delta_K (R_K(u_h), \mathbf{b} \cdot \nabla(u - I_h u))_K + \sum_{E \in \mathcal{E}_h} (R_E(u_h), u - I_h u)_E \\ &\quad + \sum_{K \in \mathcal{T}_h} 4\delta_K h_K^{-2} \varepsilon^2 c_{\text{inv}}^2 \|\nabla(u - I_h u)\|_{0,K}^2 + \sum_{K \in \mathcal{T}_h} 2\delta_K \varepsilon^2 \|\Delta(u - I_h u)\|_{0,K}^2. \end{aligned} \tag{27}$$

Now, the first three terms on the right hand side of (27) have to be bounded such that expressions with $u - I_h u$ are absorbed by the left hand side. The norm on the left hand side consists of two or three terms, respectively, see (11) and (12). Thus, there are different ways for absorbing $u - I_h u$.

Consider the first term on the right hand side of (27). In the first step of the estimate, the Cauchy–Schwarz inequality gives

$$\begin{aligned} \sum_{K \in \mathcal{T}_h} (R_K(u_h), u - I_h u)_K &\leq \sum_{K \in \mathcal{T}_h} \|R_K(u_h)\|_{0,K} \|u - I_h u\|_{0,K} \\ &= \sum_{K \in \mathcal{T}_h} \|R_K(u_h)\|_{0,K} \|v - I_h v\|_{0,K}. \end{aligned}$$

In the case (2), one can apply the interpolation estimate (6) to $\|v - I_h v\|_{0,K}$ with $s = t = 0$ and Young's inequality to get

$$\begin{aligned} \sum_{K \in \mathcal{T}_h} (R_K(u_h), u - I_h u)_K &\leq \sum_{K \in \mathcal{T}_h} C \|R_K(u_h)\|_{0,K} \|u - u_h\|_{0,K} \\ &\leq \sum_{K \in \mathcal{T}_h} \frac{C}{\mu_0} \|R_K(u_h)\|_{0,K}^2 + \frac{1}{12} \|\mu^{1/2}(u - u_h)\|_0^2. \end{aligned} \quad (28)$$

Alternatively, one can use (6) with $s = 0, t = 1$ to obtain

$$\begin{aligned} \sum_{K \in \mathcal{T}_h} (R_K(u_h), u - I_h u)_K &\leq \sum_{K \in \mathcal{T}_h} C \|R_K(u_h)\|_{0,K} h_K \|\nabla(u - u_h)\|_{0,K} \\ &\leq \sum_{K \in \mathcal{T}_h} \frac{Ch_K^2}{\varepsilon} \|R_K(u_h)\|_{0,K}^2 + \frac{\varepsilon}{12} \|\nabla(u - u_h)\|_0^2. \end{aligned} \quad (29)$$

Finally, one can try to use the term with the streamline derivative for the bound. Young's inequality yields

$$\sum_{K \in \mathcal{T}_h} (R_K(u_h), v - I_h v)_K \leq 6 \sum_{K \in \mathcal{T}_h} \delta_K \|R_K(u_h)\|_{0,K}^2 + \frac{1}{24} \sum_{K \in \mathcal{T}_h} \delta_K^{-1} \|u - I_h u\|_{0,K}^2. \quad (30)$$

Collecting the estimates (28)–(30) together with hypothesis (14) leads to

$$\begin{aligned} \sum_{K \in \mathcal{T}_h} (R_K(u_h), u - I_h u)_K &\leq \min \left\{ \frac{C}{\mu_0}, Ch_K^2 \varepsilon^{-1}, 6\delta_K \right\} \|R_K(u_h)\|_{0,K}^2 \\ &\quad + \frac{1}{12} \|u - u_h\|_{\text{SUPG}}^2. \end{aligned} \quad (31)$$

The size of the individual terms in the minimum will be discussed in Remark 4.

For estimating the second term on the right hand side of (27), first the Cauchy–Schwarz and Young's inequality are applied

$$\begin{aligned} \sum_{K \in \mathcal{T}_h} \delta_K (R_K(u_h), \mathbf{b} \cdot \nabla(u - I_h u))_K &\leq 6 \sum_{K \in \mathcal{T}_h} \delta_K \|R_K(u_h)\|_{0,K}^2 \\ &\quad + \frac{1}{24} \sum_{K \in \mathcal{T}_h} \delta_K \|\mathbf{b} \cdot \nabla(u - I_h u)\|_{0,K}^2. \end{aligned}$$

Using (15), one obtains

$$\begin{aligned} \sum_{K \in \mathcal{T}_h} \delta_K (R_K(u_h), \mathbf{b} \cdot \nabla(u - I_h u))_K &\leq 6 \sum_{K \in \mathcal{T}_h} \delta_K \|R_K(u_h)\|_{0,K}^2 + \frac{1}{12} \|u - u_h\|_{\text{SUPG}}^2. \end{aligned} \quad (32)$$

The estimate of the third term on the right hand side of (27) starts like the estimates of the other terms

$$\begin{aligned} \sum_{E \in \mathcal{E}_h} (R_E(u_h), u - I_h u)_E &\leq \sum_{E \in \mathcal{E}_h} \|R_E(u_h)\|_{0,E} \|u - I_h u\|_{0,E} \\ &= \sum_{E \in \mathcal{E}_h} \|R_E(u_h)\|_{0,E} \|v - I_h v\|_{0,E}. \end{aligned} \quad (33)$$

Using (8) and (6), the shape regularity of the mesh cells, the Cauchy–Schwarz inequality, and a straightforward estimate given in [25, Lemma 3.2], one gets

$$\begin{aligned} \|v - I_h v\|_{0,E} &\leq C \left(h_K^{-1/2} \min \{ h_K \varepsilon^{-1/2}, \mu_0^{-1/2} \} \right. \\ &\quad \times \left(\varepsilon^{1/2} \|\nabla v\|_{0,K} + \|\mu^{1/2} v\|_{0,K} \right) \\ &\quad \left. + \varepsilon^{-1/4} \min \{ h_K \varepsilon^{-1/2}, \mu_0^{-1/2} \}^{1/2} \right. \\ &\quad \times \left(\varepsilon^{1/2} \|\nabla v\|_{0,K} + \|\mu^{1/2} v\|_{0,K} \right)^{1/2} \varepsilon^{1/4} \|\nabla v\|_{0,K}^{1/2} \Big) \\ &\leq C \varepsilon^{-1/4} \min \{ h_K \varepsilon^{-1/2}, \mu_0^{-1/2} \}^{1/2} \\ &\quad \times \left(\varepsilon \|\nabla v\|_{0,K}^2 + \|\mu^{1/2} v\|_{0,K}^2 \right)^{1/2} \\ &\leq C \min \left\{ \frac{h_K^{1/2}}{\varepsilon^{1/2}}, \frac{1}{\mu_0^{1/4} \varepsilon^{1/4}} \right\} \|u - u_h\|_{\text{SUPG},K}. \end{aligned}$$

This estimate is inserted into (33) and Young's inequality is applied. A second estimate of the term on the faces can be obtained by applying first Young's inequality in (33) and afterwards (16). Using the shape regularity of the triangulation, one obtains

$$\begin{aligned} \sum_{E \in \mathcal{E}_h} (R_E(u_h), u - I_h u)_E &\leq \sum_{E \in \mathcal{E}_h} \min \left\{ \frac{6}{\|\mathbf{b}\|_{\infty,E}}, C \frac{h_E}{\varepsilon}, \frac{C}{\varepsilon^{1/2} \mu_0^{1/2}} \right\} \|R_E(u_h)\|_{0,E}^2 \\ &\quad + \frac{1}{12} \|u - u_h\|_{\text{SUPG}}^2. \end{aligned} \quad (34)$$

Theorem 1. *Let the conditions of Lemma 1 hold. Under Hypothesis 1, one gets the following global upper bound*

$$\begin{aligned} \|u - u_h\|_{\text{SUPG}}^2 &\leq \eta_1^2 + \eta_2^2 + \eta_3^2 + \sum_{K \in \mathcal{T}_h} 16\delta_K h_K^{-2} \varepsilon^2 c_{\text{inv}}^2 \|\nabla(u - I_h u)\|_{0,K}^2 \\ &\quad + \sum_{K \in \mathcal{T}_h} 8\delta_K \varepsilon^2 \|\Delta(u - I_h u)\|_{0,K}^2, \end{aligned} \quad (35)$$

where

$$\begin{aligned} \eta_1^2 &= \sum_{K \in \mathcal{T}_h} \min \left\{ \frac{C}{\mu_0}, C \frac{h_K^2}{\varepsilon}, 24\delta_K \right\} \|R_K(u_h)\|_{0,K}^2, \\ \eta_2^2 &= \sum_{K \in \mathcal{T}_h} 24\delta_K \|R_K(u_h)\|_{0,K}^2, \\ \eta_3^2 &= \sum_{E \in \mathcal{E}_h} \min \left\{ \frac{24}{\|\mathbf{b}\|_{\infty,E}}, C \frac{h_E}{\varepsilon}, \frac{C}{\varepsilon^{1/2} \mu_0^{1/2}} \right\} \|R_E(u_h)\|_{0,E}^2. \end{aligned} \quad (36)$$

Proof. The proof follows directly by inserting (31), (32) and (34) into (27). □

Remark 3 (On the additional terms on the right hand side of (35)). Besides the a posteriori terms, there are two extra terms on the right hand side of (35). It will be discussed here that these terms are in the convection-dominated regime negligible compared with the error of the SUPG approximation. This point justifies the use of the quantity $(\eta_1^2 + \eta_2^2 + \eta_3^2)^{1/2}$ as an upper error estimate.

Consider the convection-dominated regime. For the first extra term on the right hand side of (35), one obtains with (9) and (11) or (12)

$$\sum_{K \in \mathcal{T}_h} 16\delta_K h_K^{-2} \varepsilon^2 c_{\text{inv}}^2 \|\nabla(u - I_h u)\|_{0,K}^2 \leq C \sum_{K \in \mathcal{T}_h} Pe_K^{-1} \|u - I_h u\|_{\text{SUPG},K}^2. \quad (37)$$

One can expect that $\|u - I_h u\|_{\text{SUPG},K}$ is generally not much larger than $\|u - u_h\|_{\text{SUPG},K}$. Then, in the case $Pe_K \gg 1$, the right hand side of (37) becomes small compared with the left hand side of (35).

The order of convergence of the error of the SUPG approximation is $r + 1/2$, see (17). For the other additional term, one can apply (7) and (9) to get

$$\begin{aligned} \sum_{K \in \mathcal{T}_h} 8\delta_K \varepsilon^2 \|\Delta(u - I_h u)\|_{0,K}^2 &\leq C \sum_{K \in \mathcal{T}_h} \delta_K \varepsilon^2 h_K^{2r-2} \|u\|_{r+1,K}^2 \\ &\leq C \sum_{K \in \mathcal{T}_h} \|\mathbf{b}\|_{\infty,K} Pe_K^{-2} h_K^{2r+1} \|u\|_{r+1,K}^2. \end{aligned}$$

This bound possesses the same asymptotic with respect to h like the left hand side of (35) but a very small factor for $Pe_K \gg 1$. The actual size of the extra terms will be studied numerically in Example 2.

In the diffusion-dominated regime, an analysis can be performed such that there are no extra terms, see Remark 4.

Remark 4 (Comparisons with residual-based error estimators from the literature). Residual-based a posteriori error estimators for convection–diffusion–reaction equations can be obtained for different norms. With the traditional approach of deriving this kind of estimators [24] and taking care only on the dependency of the weights on the local mesh width, one gets

$$\|\nabla(u - u_h)\|_0^2 \leq C \left(\sum_{K \in \mathcal{T}_h} h_K^2 \|R_K(u_h)\|_{0,K}^2 + \sum_{E \in \mathcal{E}_h} h_E \|R_E(u_h)\|_{0,E}^2 \right) + h.o.t., \tag{38}$$

$$\|u - u_h\|_0^2 \leq C \left(\sum_{K \in \mathcal{T}_h} h_K^4 \|R_K(u_h)\|_{0,K}^2 + \sum_{E \in \mathcal{E}_h} h_E^2 \|R_E(u_h)\|_{0,E}^2 \right) + h.o.t. \tag{39}$$

The estimates (38) and (39) are not robust in the convection-dominated regime, i.e., the constants C depend on the Péclet number, cf. the numerical studies in [16]. They become robust if diffusion dominates. The higher order terms describe data approximation errors but not extra terms of the form that appear in (35).

A robust error estimator in the $L^2(\Omega)$ norm was derived in [10]. The weights in this estimator depend on the concrete finite element. Moreover, the estimator in [10] is given in terms of the $L^\infty(K)$ norm of the residual. To use a uniform framework, we consider here a counterpart of this estimator that is using the square (this gives a factor of 2 from the triangle inequality) of the $L^2(\Omega)$ norm of the local residuals. It has the form

$$\|u - u_h\|_0^2 \leq 2 \sum_{K \in \mathcal{T}_h} \left(\eta_{L^2,K}^2 \|R_K(u_h)\|_{0,K}^2 + \frac{1}{4} \sum_{E \subset \partial K} \frac{|E|}{|K|} \eta_{L^2,K}^2 \|R_E(u_h)\|_{0,E}^2 \right), \tag{40}$$

where $|E|$ and $|K|$ are the measures of E and K , respectively, and

$$\eta_{L^2,K} = \min \left\{ \frac{\tilde{h}_K}{\sqrt{2} \|\mathbf{b}\|_{L^\infty(K)}}, \frac{h_K^2}{3\sqrt{10}\varepsilon}, \frac{1}{|C|_{L^\infty(K)}} \right\}$$

for the Q_1 finite element, see [10, Appendix C]. Here, \tilde{h}_K is the cell diameter in the direction of the convection vector. The approximation sign comes not only from the transform in our framework but also from some approximation in the derivation of this estimator. Note that in the convection-dominated regime, the weights in (40) are $\mathcal{O}(h_K^2)$ for the mesh cell residuals and $\mathcal{O}(h_E)$ for the face residuals, i.e., (40) has more or less the same weights with respect to the local mesh width as (38) but both error estimators were derived for different norms.

In Verfürth [25], a non-robust residual-based error estimator for the energy norm

$$\|v\|_{\text{en}} = \left(\varepsilon \|\nabla v\|_0^2 + \|\mu^{1/2} v\|_0^2 \right)^{1/2}$$

was derived. The analysis of [25] was refined in [26], leading to a robust residual-based a posteriori error estimator for the energy norm plus a dual norm of the convective derivative

$$\begin{aligned} \|u - u_h\|_{\text{en}}^2 + \sup_{v \in H_b^1(\Omega)} \frac{\langle \mathbf{b} \cdot \nabla(u - u_h), v \rangle}{\|v\|_{\text{en}}^2} \\ \leq C \left(\sum_{K \in \mathcal{T}_h} \min \left\{ \frac{1}{\mu_0}, \frac{h_K^2}{\varepsilon} \right\} \|R_K(u_h)\|_{0,K}^2 \right. \\ \left. + \sum_{E \in \mathcal{E}_h} \min \left\{ \frac{h_E}{\varepsilon}, \frac{1}{\varepsilon^{1/2} \mu_0^{1/2}} \right\} \|R_E(u_h)\|_{0,E}^2 \right) + h.o.t. \end{aligned} \tag{41}$$

The weights of the estimators from [25,26] are the same. Note that the weights in front of the local residuals in (41) appear also in (36).

In the diffusion-dominated regime, the weights including h_K and h_E will eventually become effective in (36) and (41) such that in both cases one obtains

$$\|u - u_h\|_{\text{SUPG}}^2 \leq C \left(\sum_{K \in \mathcal{T}_h} \frac{h_K^2}{\varepsilon} \|R_K(u_h)\|_{0,K}^2 + \sum_{E \in \mathcal{E}_h} \frac{h_E}{\varepsilon} \|R_E(u_h)\|_{0,E}^2 \right) + h.o.t.$$

That means, the weights of the H^1 norm estimator (38) divided by ε are recovered. At this point, a comment about the two additional terms in (35) is in order. In the diffusion-dominated regime, the norms $\|\cdot\|_{\text{en}}$ and $\|\cdot\|_{\text{SUPG}}$ are equivalent. Then, one can apply the error bounds for the energy norm instead of the SUPG norm and following the analysis of [25,26], the two extra terms in (35) do not appear.

On the other hand, in the convection-dominated regime $Pe_K \gg 1$, the other weights $24\delta_K$ and 24 are effective in (36) since the minimum is attained at these values of the weights, hence

$$\|u - u_h\|_{\text{SUPG}}^2 \leq C \left(\sum_{K \in \mathcal{T}_h} \frac{h_K}{\|\mathbf{b}\|_{\infty,K}} \|R_K(u_h)\|_{0,K}^2 + \frac{1}{\|\mathbf{b}\|_{\infty,E}} \sum_{E \in \mathcal{E}_h} \|R_E(u_h)\|_{0,E}^2 \right) + h.o.t. \tag{42}$$

Both parts $\left(\sum_{K \in \mathcal{T}_h} \delta_K \|\mathbf{b} \cdot \nabla(u - u_h)\|_{0,K}^2 \right)^{1/2}$ and $\|\mu^{1/2}(u - u_h)\|_0$ of the SUPG error are bounded by the right hand side of (42). This estimate gives for the a posteriori bound the same difference with respect to the mesh size of order $h^{1/2}$ between the weighted $L^2(\Omega)$ norm and the $L^2(\Omega)$ norm of the streamline derivative that is known from the a priori error analysis. In the convection-dominated regime, the weights in (42) will be generally smaller than the weights of (41). Thus, the right hand side of (42) will be a smaller upper bound of the error in the energy norm compared with the right hand side of (41). Note that the scaling for the interior residual in (42) is the same as for an a posteriori error estimator of an interior penalty finite element method applied to convection-reaction equations, see [4]. The norm considered in [4] possesses also a contribution from the streamline derivative.

Remark 5 (Dimensionality considerations). Let u be a concentration with the unit (mol) or a temperature with the unit (K). Given a diffusion ε (m^2/s), a velocity field \mathbf{b} (m/s), a reaction c ($1/\text{s}$), a right hand side f (mol/s) or (K/s), and the stabilization parameters $\{\delta_K\}$ (s), a straightforward calculation reveals that both sides of estimate (35) possess the same dimension ($\text{mol}^2 \text{m}^d/\text{s}$) or ($\text{K}^2 \text{m}^d/\text{s}$). In this sense, the weights of the estimator (36) are dimensionally correct.

4. A local lower error bound

This section presents a local lower a posteriori estimate for the error in the SUPG norm. The derivation of this estimate does not require an hypothesis of the kind it was used for the global upper error bound. For the derivation of the estimate only the convection-dominated regime $Pe_K \gg 1$ will be considered, for the diffusion-dominated case see Remark 7 at the end of the section.

Bubble functions are usually applied in the derivation of local lower residual-based a posteriori error estimates. Let ψ_K be the interior bubble function associated to the mesh cell K and let ψ_E be the face bubble function associated to the face E that vanishes on the boundary of $\omega_E = K \cup K'$, where K and K' are the two mesh cells sharing the face E , see [24] for details. It is known that there exists a constant C_K independent of v and h_K such that for all polynomials v on K of degree $p \geq 0$ the following bounds hold

$$C_K^{-1} \|v\|_{0,K}^2 \leq (v, v\psi_K)_{0,K} \leq C_K \|v\|_{0,K}^2, \tag{43}$$

$$C_K^{-1} \|v\|_{0,K} \leq \|v\psi_K\|_{0,K} + h_K \|\nabla(v\psi_K)\|_{0,K} \leq C_K \|v\|_{0,K}. \tag{44}$$

For the proof of these estimates see [24], [1, Theorem 2.2]. Similar estimates hold for the face bubble functions. There exists a constant C independent of v and h_K such that for all polynomials v on K of degree $p \geq 0$ and for all $E \subset \partial K$, the following bounds

$$C^{-1} \|v\|_{0,E}^2 \leq (v, v\psi_E)_{0,E} \leq C \|v\|_{0,E}^2, \tag{45}$$

$$h_K^{-1/2} \|v\psi_E\|_{0,K} + h_K^{1/2} \|\nabla(v\psi_E)\|_{0,K} \leq C \|v\|_{0,E} \tag{46}$$

are valid. Again, the proof can be found in [24], [1, Theorem 2.4].

4.1. Interior residuals

Consider a mesh cell K and let

$$R_{K,h}(u_h) = f_h - \varepsilon u_h - \mathbf{b}_h \cdot \nabla u_h - c_h u_h$$

be a continuous approximation of the interior residual on K in a suitable finite-dimensional space, not necessarily in $V_{h,r}$, where f_h , \mathbf{b}_h , and c_h are appropriate approximations of the coefficients. Then, it follows from (43) that

$$\|R_{K,h}(u_h)\|_{0,K}^2 \leq C_K (R_{K,h}(u_h), R_{K,h}(u_h)\psi_K)_K. \quad (47)$$

Let $v = R_{K,h}(u_h)\psi_K$. This function vanishes on the boundary of K and it can be extended to the rest of the domain as a continuous function by defining its value outside K to be zero. The resulting function, again denoted by v , belongs to the space $H_D^1(\Omega)$. Using the same technique as for the derivation of (26), without applying the Galerkin orthogonality, leads to

$$a_{\text{SUPG}}(e, R_{K,h}(u_h)\psi_K) = (R_K(u_h), R_{K,h}(u_h)\psi_K)_K + \delta_K (R_K(u_h), \mathbf{b} \cdot \nabla (R_{K,h}(u_h)\psi_K))_K, \quad (48)$$

where $e = u - u_h$. From (47) and (48), one obtains

$$\begin{aligned} \|R_{K,h}(u_h)\|_{0,K}^2 &\leq C_K [(R_{K,h}(u_h) - R_K(u_h), R_{K,h}(u_h)\psi_K)_K \\ &\quad + a_{\text{SUPG}}(e, R_{K,h}(u_h)\psi_K) - \delta_K (R_K(u_h), \mathbf{b} \cdot \nabla (R_{K,h}(u_h)\psi_K))_K] \\ &= C_K [(R_{K,h}(u_h) - R_K(u_h), R_{K,h}(u_h)\psi_K)_K \\ &\quad + a_{\text{SUPG}}(e, R_{K,h}(u_h)\psi_K) \\ &\quad - \delta_K ((R_K(u_h) - R_{K,h}(u_h)), \mathbf{b} \cdot \nabla (R_{K,h}(u_h)\psi_K))_K \\ &\quad - \delta_K (R_K(u_h), \mathbf{b} \cdot \nabla (R_{K,h}(u_h)\psi_K))_K]. \end{aligned} \quad (49)$$

The terms on the right hand side of (49) have to be bounded. Besides the Cauchy–Schwarz inequality or Hölder’s inequality, estimate (44) will be used. One gets for the first term

$$\begin{aligned} &|(R_{K,h}(u_h) - R_K(u_h), R_{K,h}(u_h)\psi_K)_{0,K}| \\ &\leq \|\psi_K R_{K,h}(u_h)\|_{0,K} \|R_{K,h}(u_h) - R_K(u_h)\|_{0,K} \\ &\leq C_K \|R_{K,h}(u_h)\|_{0,K} \|R_{K,h}(u_h) - R_K(u_h)\|_{0,K}. \end{aligned} \quad (50)$$

For the third term, one obtains with (9)

$$\begin{aligned} &|-\delta_K ((R_K(u_h) - R_{K,h}(u_h)), \mathbf{b} \cdot \nabla (R_{K,h}(u_h)\psi_K))_K| \\ &\leq \delta_K \|R_K(u_h) - R_{K,h}(u_h)\|_{0,K} \|\mathbf{b}\|_{\infty,K} \|\nabla (R_{K,h}(u_h)\psi_K)\|_{0,K} \\ &\leq C_K \delta_K h_K^{-1} \|\mathbf{b}\|_{\infty,K} \|R_{K,h}(u_h) - R_K(u_h)\|_{0,K} \|R_{K,h}(u_h)\|_{0,K} \\ &\leq \frac{1}{2C_K} \|R_{K,h}(u_h) - R_K(u_h)\|_{0,K} \|R_{K,h}(u_h)\|_{0,K} \end{aligned} \quad (51)$$

and for the fourth term

$$\begin{aligned} &|-\delta_K (R_{K,h}(u_h), \mathbf{b} \cdot \nabla (R_{K,h}(u_h)\psi_K))_K| \\ &\leq \delta_K \|R_{K,h}(u_h)\|_{0,K} \|\mathbf{b}\|_{\infty,K} \|\nabla (R_{K,h}(u_h)\psi_K)\|_{0,K} \\ &\leq C_K \delta_K h_K^{-1} \|\mathbf{b}\|_{\infty,K} \|R_{K,h}(u_h)\|_{0,K} \leq \frac{1}{2C_K} \|R_{K,h}(u_h)\|_{0,K}^2. \end{aligned} \quad (52)$$

The goal of estimating the second term on the right hand side of (49) consists in introducing the SUPG norm of the error. To this end, the estimate starts with

$$\begin{aligned} |a_{\text{SUPG}}(e, R_{K,h}(u_h)\psi_K)| &\leq \varepsilon^{1/2} \|\nabla e\|_{0,K} \varepsilon^{1/2} \|\nabla (R_{K,h}(u_h)\psi_K)\|_{0,K} \\ &\quad + \delta_K^{1/2} \|\mathbf{b} \cdot \nabla e\|_{0,K} \delta_K^{-1/2} \|R_{K,h}(u_h)\psi_K\|_{0,K} \\ &\quad + \|\mu^{1/2} e\|_{0,K} \|c\|_{\infty,K} \mu_0^{-1/2} \|R_{K,h}(u_h)\psi_K\|_{0,K} \\ &\quad + \delta_K \varepsilon \|\Delta e\|_{0,K} \|\mathbf{b}\|_{\infty,K} \|\nabla (R_{K,h}(u_h)\psi_K)\|_{0,K} \\ &\quad + \delta_K^{1/2} \|\mathbf{b} \cdot \nabla e\|_{0,K} \delta_K^{1/2} \|\mathbf{b}\|_{\infty,K} \|\nabla (R_{K,h}(u_h)\psi_K)\|_{0,K} \\ &\quad + \|\mu^{1/2} e\|_{0,K} \delta_K \|c\|_{\infty,K} \mu_0^{-1/2} \|\mathbf{b}\|_{\infty,K} \\ &\quad \times \|\nabla (R_{K,h}(u_h)\psi_K)\|_{0,K}. \end{aligned} \quad (53)$$

Note that the terms with $\mu_0^{-1/2}$ are not there if $\mu_0 = 0$ since then the reactive term is not present, see (3). Using the inverse inequality (5), one gets

$$\begin{aligned} \|\Delta e\|_{0,K} &\leq \|\Delta(u - I_h u)\|_{0,K} + \|\Delta(I_h u - u_h)\| \\ &\leq \|\Delta(u - I_h u)\|_{0,K} + c_{\text{inv}} h_K^{-1} \|\nabla(I_h u - u_h)\|_{0,K} \\ &\leq \|\Delta(u - I_h u)\|_{0,K} + c_{\text{inv}} h_K^{-1} (\|\nabla e\|_{0,K} + \|\nabla(u - I_h u)\|_{0,K}). \end{aligned}$$

Inserting this estimate into (53), applying (44), and rearranging terms leads to

$$\begin{aligned} |a_{\text{SUPG}}(e, R_{K,h}(u_h)\psi_K)| &\leq \left[(\varepsilon^{1/2} C_K h_K^{-1} \|\mathbf{b}\|_{\infty,K}^{-1/2} + \varepsilon^{1/2} \delta_K h_K^{-2} c_{\text{inv}} C_K \right. \\ &\quad \times \|\mathbf{b}\|_{\infty,K}^{1/2}) \|\mathbf{b}\|_{\infty,K}^{1/2} \varepsilon^{1/2} \|\nabla e\|_{0,K} + (\|c\|_{\infty,K} \mu_0^{-1/2} C_K \\ &\quad \times \|\mathbf{b}\|_{\infty,K}^{-1/2} + \delta_K \mu_0^{-1/2} \|c\|_{\infty,K} C_K h_K^{-1} \|\mathbf{b}\|_{\infty,K}^{1/2}) \\ &\quad \times \|\mathbf{b}\|_{\infty,K}^{1/2} \mu^{1/2} e\|_{0,K} + (\delta_K^{-1/2} C_K \|\mathbf{b}\|_{\infty,K}^{-1/2} \\ &\quad + \delta_K^{1/2} h_K^{-1} C_K \|\mathbf{b}\|_{\infty,K}^{1/2}) \delta_K^{1/2} \|\mathbf{b}\|_{\infty,K}^{1/2} \|\mathbf{b} \cdot \nabla e\|_{0,K} \\ &\quad + \varepsilon h_K^{-1/2} \|\nabla(u - I_h u)\|_{0,K} (\delta_K C_K h_K^{-3/2} \|\mathbf{b}\|_{\infty,K} c_{\text{inv}}) \\ &\quad \left. + \varepsilon h_K^{1/2} \|\Delta(u - I_h u)\|_{0,K} (\delta_K C_K h_K^{-3/2} \|\mathbf{b}\|_{\infty,K}) \right] \\ &\quad \times \|R_{K,h}(u_h)\|_{0,K}. \end{aligned} \quad (54)$$

Let $\tilde{\alpha}_K$ be the maximum of the terms in parentheses in (54), i.e.

$$\tilde{\alpha}_K = \max \left\{ (\varepsilon^{1/2} C_K h_K^{-1} \|\mathbf{b}\|_{\infty,K}^{-1/2} + \varepsilon^{1/2} \delta_K h_K^{-2} c_{\text{inv}} C_K \|\mathbf{b}\|_{\infty,K}^{1/2}), (\dots), (\dots) \right\}$$

and set $\alpha_K = \sqrt{3} \tilde{\alpha}_K$. Then, it follows that

$$\begin{aligned} |a_{\text{SUPG}}(e, R_{K,h}(u_h)\psi_K)| &\leq \left[\alpha_K \|\mathbf{b}\|_{\infty,K}^{1/2} \|e\|_{\text{SUPG},K} \right. \\ &\quad \left. + \tilde{\alpha}_K (\varepsilon h_K^{-1/2} \|\nabla(u - I_h u)\|_{0,K} + \varepsilon h_K^{1/2} \|\Delta(u - I_h u)\|_{0,K}) \right] \|R_{K,h}(u_h)\|_{0,K}. \end{aligned} \quad (55)$$

Inserting (50), (51), (52), and (55) into (49) leads to

$$\begin{aligned} \frac{1}{2} \|R_{K,h}(u_h)\|_{0,K} &\leq C_K \alpha_K \|\mathbf{b}\|_{\infty,K}^{1/2} \|e\|_{\text{SUPG},K} \\ &\quad + \left(C_K^2 + \frac{1}{2} \right) \|R_{K,h}(u_h) - R_K(u_h)\|_{0,K} \\ &\quad + C_K \tilde{\alpha}_K (\varepsilon h_K^{-1/2} \|\nabla(u - I_h u)\|_{0,K} + \varepsilon h_K^{1/2} \|\Delta(u - I_h u)\|_{0,K}). \end{aligned} \quad (56)$$

Using (9), an inspection of the individual terms of α_K and, consequently, $\tilde{\alpha}_K$ gives that $\alpha_K \leq Ch_K^{-1/2}$ and $\tilde{\alpha}_K \leq Ch_K^{-1/2}$ (note that $\alpha_K, \tilde{\alpha}_K$ have the correct unit ($\text{m}^{-1/2}$)). Denoting by

$$\eta_{\text{int},K} := \frac{h_K^{1/2}}{\|\mathbf{b}\|_{\infty,K}^{1/2}} \|R_K(u_h)\|_{0,K}, \quad (57)$$

one obtains from (56) with the help of the triangle inequality

$$\begin{aligned} \eta_{\text{int},K} &\leq C \|e\|_{\text{SUPG},K} + \frac{C}{\|\mathbf{b}\|_{\infty,K}^{1/2}} \left[h_K^{1/2} (\|f - f_h\|_{0,K} + \|(\mathbf{b} - \mathbf{b}_h) \cdot \nabla u_h\|_{0,K} \right. \\ &\quad \left. + \|(c - c_h)u_h\|_{0,K}) + \varepsilon h_K^{-1/2} \|\nabla(u - I_h u)\|_{0,K} + \varepsilon h_K^{1/2} \|\Delta(u - I_h u)\|_{0,K} \right]. \end{aligned} \quad (58)$$

Note that for δ_K as defined in (9) the local error estimator $\eta_{\text{int},K}$ is of the form as the local contribution η_2 of the global error estimator, see (36). If the minimum of the terms in η_1 is the last term, which will be the case in the convection-dominated regime, cf. Remark 4, then also the local contribution of η_1 is of the same form as $\eta_{\text{int},K}$.

Remark 6 (On the additional terms on the right hand side of (58)). The application of (6) yields

$$\begin{aligned} \varepsilon h_K^{-1/2} \|\nabla(u - I_h u)\|_{0,K} &\leq C \varepsilon h_K^{-1/2} h_K^r \|u\|_{r+1,K} \\ &\leq C \|\mathbf{b}\|_{\infty,K} Pe_K^{-1} h_K^{r+1/2} \|u\|_{r+1,K} \end{aligned} \quad (59)$$

and using (7) the same bound is valid for the other term

$$\begin{aligned} \varepsilon h_K^{1/2} \|\Delta(u - I_h u)\|_{0,K} &\leq C \varepsilon h_K^{1/2} h_K^{r-1} \|u\|_{r+1,K} \\ &\leq C \|\mathbf{b}\|_{\infty,K} Pe_K^{-1} h_K^{r+1/2} \|u\|_{r+1,K}. \end{aligned} \quad (60)$$

Reasoning in the same way like for the second term in Remark 3, one finds that (59) and (60) are in the convection-dominated regime $Pe_K \gg 1$ negligible compared with $\|e\|_{\text{SUPG},K}$. The other additional terms in (58) are just the usual data approximation errors. In practice, one has to take care that the data are approximated sufficiently well such that these terms are also negligible compared with $\|e\|_{\text{SUPG},K}$. Then, $\eta_{\text{int},K}$ is the first contribution of a local a posteriori error estimator.

4.2. Face residuals

The analysis of the face residuals follows in principal the analysis of the interior residuals. Let $R_{E,h}(u_h)$ be an approximation to the face residual from a suitable finite-dimensional space. Then, one obtains with (45)

$$\|R_{E,h}(u_h)\|_{0,E}^2 \leq C (R_{E,h}(u_h), R_{E,h}(u_h)\psi_E). \quad (61)$$

Now, the function $v = R_{E,h}(u_h)\psi_E$ is defined, which is continuous and which vanishes on the boundary of ω_E . This function can be extended by zero to Ω such that a function $v \in H_0^1(\Omega)$ is obtained. Inserting v into the analog of (26), which is obtained without the application of the Galerkin orthogonality, gives

$$\begin{aligned} a_{\text{SUPG}}(e, R_{E,h}(u_h)\psi_E) &= \sum_{K \in \omega_E} (R_K(u_h), R_{E,h}(u_h)\psi_E)_K \\ &\quad + \sum_{K \in \omega_E} \delta_K (R_K(u_h), \mathbf{b} \cdot \nabla (R_{E,h}(u_h)\psi_E))_K \\ &\quad + (R_E(u_h), R_{E,h}(u_h)\psi_E)_{0,E}. \end{aligned} \quad (62)$$

From (61) and (62), one gets

$$\begin{aligned} \|R_{E,h}(u_h)\|_{0,E}^2 &\leq C \left[(R_{E,h}(u_h) - R_E(u_h), R_{E,h}(u_h)\psi_E)_{0,E} + a_{\text{SUPG}}(e, R_{E,h}(u_h)\psi_E) \right. \\ &\quad - \sum_{K \in \omega_E} (R_K(u_h), R_{E,h}(u_h)\psi_E)_K \\ &\quad \left. - \sum_{K \in \omega_E} \delta_K (R_K(u_h), \mathbf{b} \cdot \nabla (R_{E,h}(u_h)\psi_E))_K \right]. \end{aligned} \quad (63)$$

The four terms on the right hand side of (63) have to be bounded. Applying the Cauchy–Schwarz inequality and (45) yields

$$\begin{aligned} &|(R_{E,h}(u_h) - R_E(u_h), R_{E,h}(u_h)\psi_E)_{0,E}| \\ &\leq \|R_{E,h}(u_h)\psi_E^{1/2}\|_{0,E} \|(R_{E,h}(u_h) - R_E(u_h))\psi_E^{1/2}\|_{0,E} \\ &\leq C \|R_{E,h}(u_h)\|_{0,E} \|(R_{E,h}(u_h) - R_E(u_h))\|_{0,E}. \end{aligned} \quad (64)$$

For estimating the third and fourth term on the right hand side of (63), inequality (46) is applied

$$\begin{aligned} \left| \sum_{K \in \omega_E} (R_K(u_h), R_{E,h}(u_h)\psi_E)_K \right| &\leq \sum_{K \in \omega_E} \|R_K(u_h)\|_{0,K} \|R_{E,h}(u_h)\psi_E\|_{0,K} \\ &\leq C \left(\sum_{K \in \omega_E} h_K^{1/2} \|R_K(u_h)\|_{0,K} \right) \|R_{E,h}(u_h)\|_{0,E} \end{aligned} \quad (65)$$

and

$$\begin{aligned} &\left| \sum_{K \in \omega_E} \delta_K (R_K(u_h), \mathbf{b} \cdot \nabla (R_{E,h}(u_h)\psi_E))_K \right| \\ &\leq \sum_{K \in \omega_E} \delta_K \|R_K(u_h)\|_{0,K} \|\mathbf{b}\|_{\infty,K} \|\nabla (R_{E,h}(u_h)\psi_E)\|_{0,K} \\ &\leq C \left(\sum_{K \in \omega_E} \delta_K h_K^{-1/2} \|R_K(u_h)\|_{0,K} \|\mathbf{b}\|_{\infty,K} \right) \|R_{E,h}(u_h)\|_{0,E} \\ &\leq C \left(\sum_{K \in \omega_E} h_K^{1/2} \|R_K(u_h)\|_{0,K} \right) \|R_{E,h}(u_h)\|_{0,E}, \end{aligned} \quad (66)$$

where in the last estimate the definition (9) of δ_K has been used. Finally, the definition of $a_{\text{SUPG}}(\cdot, \cdot)$, (54) and (46) give for the second term on the right hand side of (63)

$$\begin{aligned} |a_{\text{SUPG}}(e, R_{E,h}(u_h)\psi_E)| &\leq C \sum_{K \in \omega_E} \left[\|\mathbf{b}\|_{\infty,K}^{1/2} \varepsilon^{1/2} \|\nabla e\|_{0,K} \left(\varepsilon^{1/2} h_K^{-1/2} \|\mathbf{b}\|_{\infty,K}^{-1/2} \right. \right. \\ &\quad \left. \left. + \varepsilon^{1/2} \delta_K h_K^{-3/2} c_{\text{inv}} \|\mathbf{b}\|_{\infty,K}^{1/2} \right) + \delta_K^{1/2} \|\mathbf{b}\|_{\infty,K}^{1/2} \|\mathbf{b} \cdot \nabla e\|_{0,K} \left(\delta_K^{-1/2} h_K^{1/2} \|\mathbf{b}\|_{\infty,K}^{-1/2} \right. \right. \\ &\quad \left. \left. + \delta_K^{1/2} h_K^{-1/2} \|\mathbf{b}\|_{\infty,K}^{1/2} \right) + \|\mathbf{b}\|_{\infty,K}^{1/2} \mu^{1/2} e\|_{0,K} \left(h_K^{1/2} \mu_0^{-1/2} \|c\|_{\infty,K} \|\mathbf{b}\|_{\infty,K}^{-1/2} \right. \right. \\ &\quad \left. \left. + \delta_K h_K^{-1/2} \mu_0^{-1/2} \|c\|_{\infty,K} \|\mathbf{b}\|_{\infty,K}^{1/2} \right) + \varepsilon h_K^{-1/2} \|\nabla(u - I_h u)\|_{0,K} \right. \\ &\quad \left. \times \left(\delta_K h_K^{-1} \|\mathbf{b}\|_{\infty,K} c_{\text{inv}} \right) + \varepsilon h_K^{1/2} \|\Delta(u - I_h u)\|_{0,K} \left(\delta_K h_K^{-1} \|\mathbf{b}\|_{\infty,K} \right) \right] \\ &\quad \times \|R_{E,h}(u_h)\|_{0,E}. \end{aligned} \quad (67)$$

In the case $\mu_0 = 0$, the same remark holds as given after (53). Note that for δ_K as defined in (9) all terms in parentheses in (67) are dimensionless and $\mathcal{O}(1)$ with respect to h_K . Using the definition of $\|\cdot\|_{\text{SUPG}}$, one gets

$$\begin{aligned} |a_{\text{SUPG}}(e, R_{E,h}(u_h)\psi_E)| &\leq C \left[\sum_{K \in \omega_E} \|\mathbf{b}\|_{\infty,K}^{1/2} \|e\|_{\text{SUPG},K} + \sum_{K \in \omega_E} \varepsilon h_K^{-1/2} \|\nabla(u - I_h u)\|_{0,K} \right. \\ &\quad \left. + \sum_{K \in \omega_E} \varepsilon h_K^{1/2} \|\Delta(u - I_h u)\|_{0,K} \right] \|R_{E,h}(u_h)\|_{0,E}. \end{aligned} \quad (68)$$

Inserting (64)–(66) and (68) into (63) yields

$$\begin{aligned} \|R_{E,h}(u_h)\|_{0,E} &\leq C \left[\sum_{K \in \omega_E} \|\mathbf{b}\|_{\infty,K}^{1/2} \|e\|_{\text{SUPG},K} + \|R_{E,h}(u_h) - R_E(u_h)\|_{0,E} \right. \\ &\quad \left. + \sum_{K \in \omega_E} h_K^{1/2} \|R_K(u_h)\|_K + \sum_{K \in \omega_E} \varepsilon h_K^{-1/2} \|\nabla(u - I_h u)\|_{0,K} \right. \\ &\quad \left. + \varepsilon h_K^{1/2} \|\Delta(u - I_h u)\|_{0,K} \right]. \end{aligned} \quad (69)$$

The term $\|R_{E,h}(u_h) - R_E(u_h)\|_{0,E}$ vanishes on the interior faces and it reduces to $g - g_h$ on the Neumann boundary, where g_h is a finite dimensional approximation to g . Denoting by

$$\eta_{\text{edge},E} := \frac{1}{\|\mathbf{b}\|_{\infty,\omega_E}^{1/2}} \|R_E(u_h)\|_{0,E} \quad (70)$$

and using the definition (57), one gets from (69)

$$\begin{aligned} \eta_{\text{edge},E} &\leq C \left(\sum_{K \in \omega_E} \|e\|_{\text{SUPG},K} + \sum_{K \in \omega_E} \eta_{\text{int},K} \right) + \frac{C}{\|\mathbf{b}\|_{\infty,\omega_E}^{1/2}} \left(\sum_{E \subset \partial K, E \in \mathcal{E}_{h,N}} \|g - g_h\|_{0,E} \right. \\ &\quad \left. + \sum_{K \in \omega_E} \varepsilon h_K^{-1/2} \|\nabla(u - I_h u)\|_{0,K} + \varepsilon h_K^{1/2} \|\Delta(u - I_h u)\|_{0,K} \right). \end{aligned} \quad (71)$$

The last two terms on the right hand side of (71) can be bounded in the same way the bounds of (59) and (60) were derived. It can be observed that in the convection-dominated regime the term $\eta_{\text{edge},E}$ from (70) is of the same principal form as η_3 from (36).

Theorem 2. Consider the convection-dominated regime $Pe_K \gg 1$, let $K \in \mathcal{T}_h$, let the stabilization parameter be defined by (9), and let $u \in H^{r+1}(\omega_K)$. Then the following local lower a posteriori estimate holds

$$\begin{aligned} \eta_{\text{int},K}^2 + \sum_{E \in \partial K} \eta_{\text{edge},E}^2 &\leq C \|e\|_{\text{SUPG},\omega_K}^2 + C \sum_{K \in \omega_K} \frac{h_K}{\|\mathbf{b}\|_{\infty,K}} \left(\|f - f_h\|_{0,K}^2 \right. \\ &\quad \left. + \|(\mathbf{b} - \mathbf{b}_h) \cdot \nabla u_h\|_{0,K}^2 + \|(c - c_h)u_h\|_{0,K}^2 \right) \\ &\quad + C \sum_{E \subset \partial K, E \in \mathcal{E}_{h,N}} \frac{1}{\|\mathbf{b}\|_{\infty,\omega_E}} \|g - g_h\|_{0,E}^2 \\ &\quad + C \sum_{K \in \omega_K} \|\mathbf{b}\|_{\infty,K} Pe_K^{-2} h_K^{2r+1} \|u\|_{r+1,K}^2. \end{aligned}$$

Proof. The estimate is obtained by combining (58) and (71). \square

Remark 7. Note that in the derivation of this estimate only the convection-dominated regime was considered. Unlike the global error estimator, there is no transition of the weights in the case that the local mesh Péclet number becomes smaller, see Remark 4. However, this situation has to be faced for adaptively refined grids. Since the norms $\|\cdot\|_{\text{en}}$ and $\|\cdot\|_{\text{SUPG}}$ are equivalent in the diffusion-dominated regime, it is reasonable to use the same weights as for the estimator (41) in this regime. For this reason, we propose to use as local estimator the local counterpart of the global estimator

$$\begin{aligned} &\left(\min \left\{ \frac{C}{\mu_0}, C \frac{h_K^2}{\varepsilon}, 24\delta_K \right\} \|R_K(u_h)\|_{0,K}^2 + 24\delta_K \|R_K(u_h)\|_{0,K}^2 \right. \\ &\quad \left. + \sum_{E \in \partial K} \min \left\{ \frac{24}{\|\mathbf{b}\|_{\infty,E}}, C \frac{h_E}{\varepsilon}, \frac{C}{\varepsilon^{1/2} \mu_0^{1/2}} \right\} \|R_E(u_h)\|_{0,E}^2 \right)^{1/2}. \end{aligned} \quad (72)$$

Note that for simplifying the implementation, in the last weight $\|\mathbf{b}\|_{\infty,E}$ instead of $\|\mathbf{b}\|_{\infty,\omega_E}$ is used.

5. Numerical studies

The numerical studies will present, on the one hand, results with respect to the effectivity of the error estimators (35) and (36), the fulfillment of the hypotheses (14)–(16), and the size of the extra terms on the right hand side of estimate (35). On the other hand, the adaptive grid refinement controlled by the local estimator (72) will be compared with the refinements obtained with the other residual-based estimators from Remark 4.

A comprehensive discussion concerning possible choices of the SUPG stabilization parameter can be found in [17]. In the numerical studies presented below, the same choice of this parameter as in [17] was used

$$\delta_K = \frac{\tilde{h}_K}{2r|\mathbf{b}|} \zeta(\tilde{Pe}_K) \quad \text{with} \quad \zeta(\alpha) = \coth \alpha - \frac{1}{\alpha}, \quad \tilde{Pe}_K = \frac{|\mathbf{b}|\tilde{h}_K}{2r\varepsilon},$$

where \tilde{h}_K is the cell diameter in the direction of the convection vector \mathbf{b} , like in the weight of (40), and $|\mathbf{b}|$ is the Euclidean norm of this vector. The arising linear systems of equations were either solved with the direct sparse solver UMFPACK [6] or with a flexible GMRES method with multigrid preconditioner until the Euclidean norm of the residual vector was less than 10^{-14} . All simulations were performed with the code MoonMMD [19].

A posteriori error estimators should, on the one hand, estimate the error in a certain norm. The quality of the fulfillment of this task is usually measured by the effectivity index

$$\eta_{\text{eff}} = \frac{\eta}{\|u - u_h\|},$$

where η is the computed error estimate and $\|\cdot\|$ is the norm the estimator is designed for. For the proposed error estimator, it is

$$\eta = (\eta_1^2 + \eta_2^2 + \eta_3^2)^{1/2}, \quad (73)$$

where η_1, η_2, η_3 are given in (36). The constants in η_1 and η_3 were chosen to be $C = 1$, also for the lower estimator (72). Note that the choice of the constant C is relevant only in the diffusion-dominated regime. A reason to choose the constants in this way is that one obtains the same weights as in the error estimator (41). On the other hand, a posteriori error estimators should control an adaptive grid refinement. There are several strategies for utilizing local error estimates in this process, see [16] for a discussion of this topic. Here, the same strategy as in [16] was used. After having computed the local error estimates, e.g. (72), for all mesh cells, the maximal value $\bar{\eta}$ was determined. Then, all mesh cells were refined whose local estimate is at least $\text{tol} = 0.5$ of $\bar{\eta}$. For efficiency reasons, tol was decreased by 0.9 as long as less than 10% of the mesh cells were marked for refinement. It turned out that in all simulations the minimal amount of mesh cells that should be refined became effective such that the initial value for tol was of little importance.

Example 1 (Smooth solution). This example studies the effectivity of the a posteriori error estimator (73) for the diffusion- and convection-dominated regime. To this end, Eq. (1) is considered in $\Omega = (0, 1)^2$ with $\mathbf{b} = (1, -4)^T$, $c = 1$, and with f chosen such that $u(x, y) = \sin(\pi x) \sin(\pi y)$

is the solution of (1). Dirichlet boundary conditions were prescribed at $x = 0$, $y = 0$, and $y = 1$. At $x = 1$, Neumann boundary conditions were applied.

Uniformly refined grids were used in the simulations. The coarsest grids (level 0) are presented in Fig. 1. The finest grid in all simulations was the first grid with more than 10^6 degrees of freedom. Simulations were performed for first, second, and third order finite elements.

Results with respect to the effectivity index for different finite elements and different diffusion parameters ε are presented in Fig. 2. In all cases, the effectivity index is in the interval [5, 12]. Considering only the convection-dominated case, then the effectivity index is always in the interval [6.5, 7]. In summary, one can observe that the effectivity index behaves robustly with respect to the Péclet number.

In our studies, we could observe that also the $L^2(\Omega)$ error estimator (40) was robust, whereas the error estimators for the H^1 norm (38), the L^2 norm (39), and the energy norm estimator from [25] do not possess this property even in this example with a smooth solution, see also [16] for corresponding studies.

Finally, it shall be noted that the hypotheses (14)–(16) were always fulfilled in the convection-dominated regime. Only in two simulations with $\nu = 1$ and $\nu = 10^{-2}$, the factor of 2.1 instead of 2 would have been necessary on the right hand side of (14). However, in the diffusion-dominated regime, the weights which are based on hypotheses (14)–(16) are not effective in the error estimator (35) and (36). For the sake of brevity, detailed results concerning this topic will be presented only in Example 2.

Example 2 (Solution with circular interior layer). This example was proposed in [15] and it is defined by $\Omega = (0, 1)^2$, $\varepsilon = 10^{-4}$, $\mathbf{b} = (2, 3)^T$, $c = 2$, and f such that

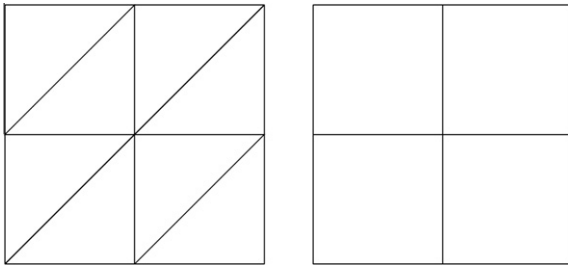


Fig. 1. Coarsest grids for the simulations on the unit square.

$$u(x, y) = 16x(1 - x)y(1 - y) \times \left(\frac{1}{2} + \frac{\arctan[2\varepsilon^{-1/2}(0.25^2 - (x - 0.5)^2 - (y - 0.5)^2)]}{\pi} \right)$$

satisfies (1), see Fig. 3. Dirichlet conditions were applied at the whole boundary. It has been recently observed in [18] that the diffusion should not be chosen too small in this example. Otherwise, the quadrature error of the right hand side term of the finite element problem might dominate. For this reason, the same diffusion $\varepsilon = 10^{-4}$ and the same quadrature rules were used as in [18].

Solutions on adaptively refined grids were studied in this example. The coarse grids from Fig. 1 were used and uniform grid refinement was applied until the first grid with more than 250 degrees of freedom was obtained. Starting from this grid, local adaption in the way described above was applied. The solution process was stopped after having computed the solution on the first grid with more than 10^5 degrees of freedom.

Snapshots of the adaptively refined grids using the local estimator (72) for the P_1 finite element are presented in Fig. 4. For quadrilateral grids, an adaptive refinement with hanging nodes was applied. The effectivity indices on adaptively refined grids for different finite elements are presented in Fig. 5. One can observe a very similar behavior as in Example 1. Starting from the second coarsest grid, the indices are always in the interval [6.5,7]. In addition, we could observe that the proposed error estimator (35) and (36) is robust in estimating the error in the SUPG norm also on the grids obtained with the other estimators.

A study of quantities involved in hypotheses (14)–(16) is presented in Fig. 6, where for the sake of brevity only one result is presented for each finite element of order higher than one. It can be seen that for this example the hypotheses were almost always fulfilled, there is only one exception for the Q_3 finite element on the third coarsest grid. But this is the only exception on the meshes obtained with (72), it is very small, and the quadrature error might

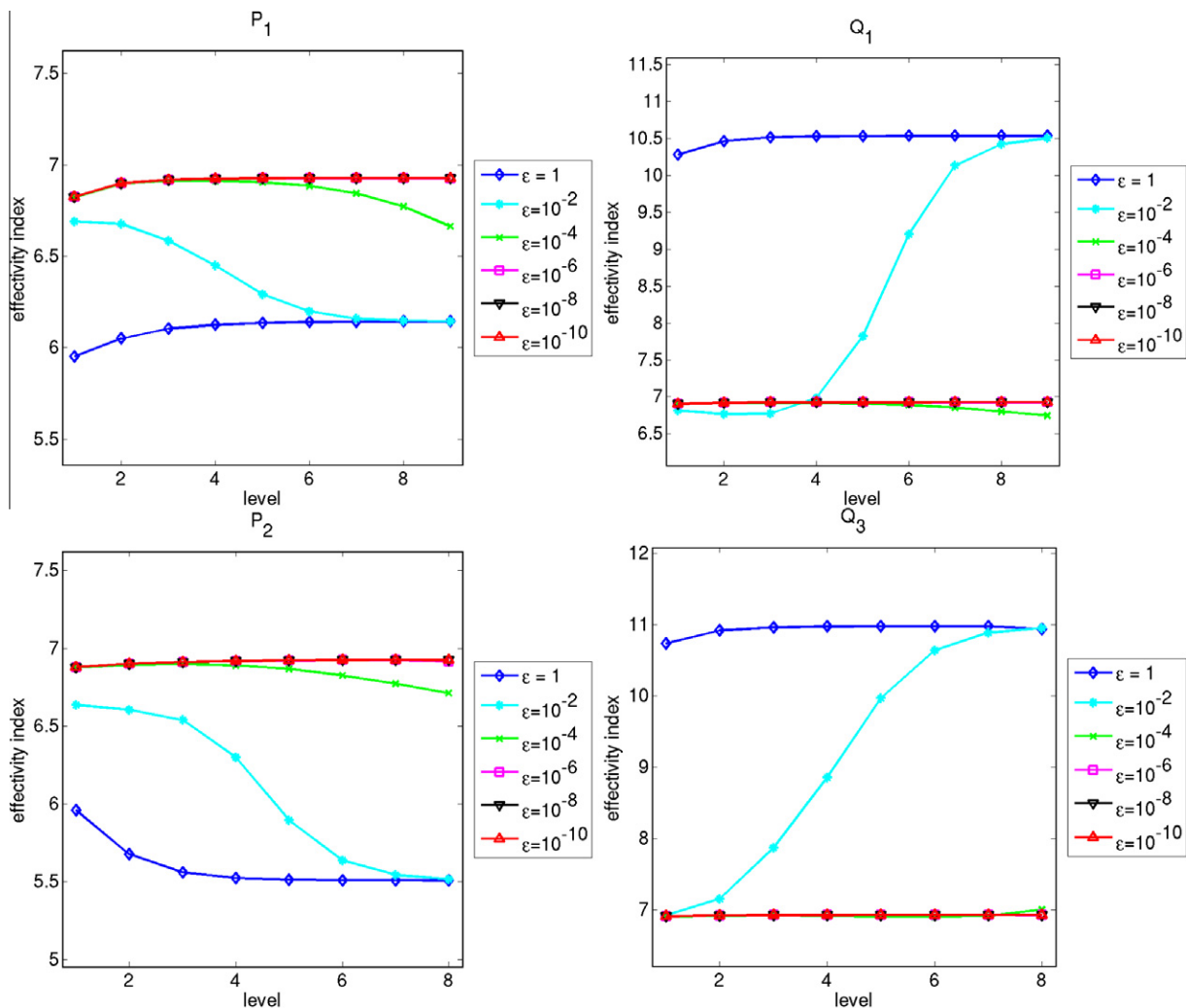


Fig. 2. Example 1. Effectivity index for different values of the diffusion and for different finite elements.

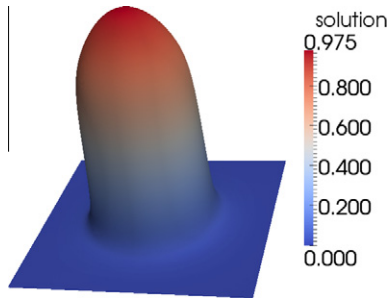


Fig. 3. Solution of Example 2.

still have some non-negligible influence on this coarse grid. In our opinion, it can be seen that hypotheses (14)–(16) are quite reasonable.

Two representative results concerning the size of the extra terms on the right hand side of estimate (35) are shown in Fig. 7. For the constant from the inverse inequality for different finite elements, values from [7] were used. It can be observed that these terms are very small for large Péclet numbers compared with the error (and thus also with the error estimator). On finer grids, the extra terms become more important which follows also from the considerations in Remark 3.

The considered example possesses only one layer. All estimators lead more or less to the same type of adaptive refinement. Instead of presenting visualizations of grids, this statement will be illustrated by the fact that the solutions computed on the adaptively refined grids obtained with the (local counterparts of the) error estimators (38)–(41) and (72) possess a very similar error in the SUPG norm, see Fig. 8 for some representative results.

Example 3 (Hemker problem). The Hemker problem, defined in [11], is a simple two-dimensional model of the transport of temperature from a hot obstacle (circle) in the direction of a constant convection field. It possesses a number of properties which are encountered also in problems coming from applications, see [2] for a discussion of this topic. From the point of view of adaptive grid refinement, the interesting property of the Hemker problem is the appearance of different layers: boundary layers at the circle and interior layers starting from the circle and evolving in the direction of the convection. The Hemker problem has been studied recently in [2] for a number of stabilized discretizations and the current study will follow the lines of [2].

The Hemker problem is defined in $\Omega = \{[-3, 9] \times [-3, 3] \setminus \{(x, y) : x^2 + y^2 < 1\}\}$, the coefficients of (1) are $\varepsilon = 10^{-4}$, $\mathbf{b} = (1, 0)^T$, $c = 0$, and $f = 0$, and the boundary conditions are given by

$$u(x, y) = \begin{cases} 0, & \text{for } x = -3, \\ 1, & \text{for } x^2 + y^2 = 1, \\ \varepsilon \nabla u \cdot \mathbf{n} = 0, & \text{else,} \end{cases}$$

see Fig. 9 for the solution of this problem.

For assessing numerical solutions of the Hemker problem, not errors in Sobolev spaces or in the SUPG norm are of interest. Instead, quantities like the size of spurious oscillations or the smearing of layers are important. None of the considered error estimators in this paper is designed to adapt the grids with respect to such outputs of interest. Based on the experience from [16], it can be expected that error estimator will lead to the best grids which adapts the grids most uniformly, since this strategy minimizes the probability of neglecting the refinement of an important subregion.

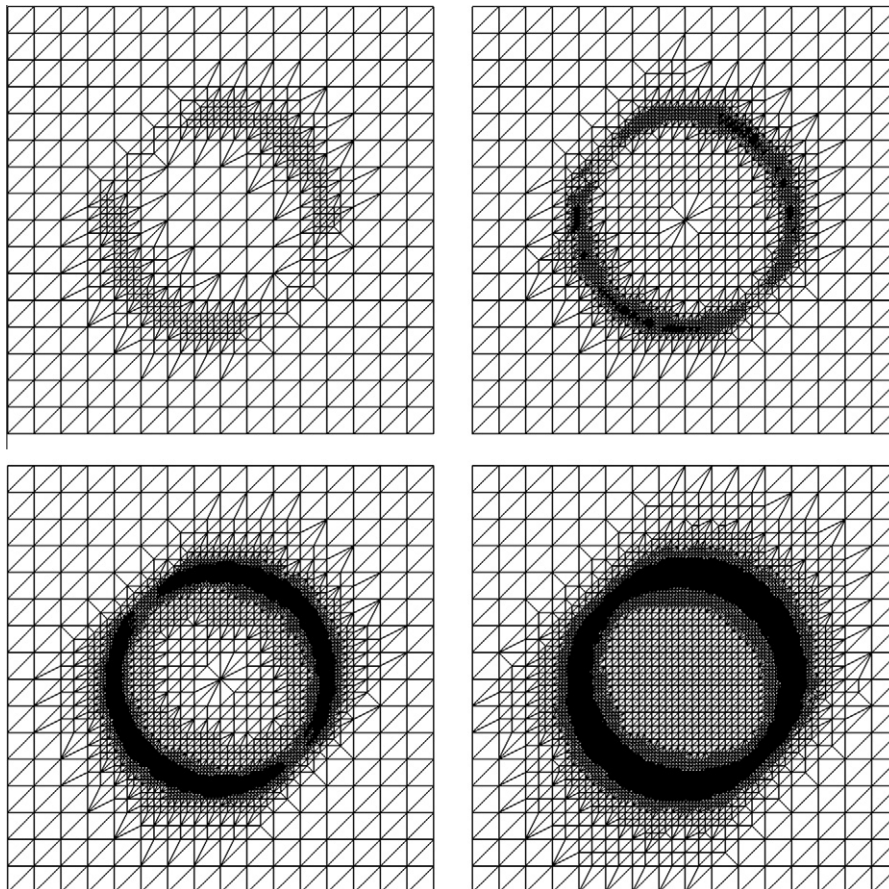


Fig. 4. Example 2. Adaptively refined grids obtained by using the local estimator (72), P_1 finite element.

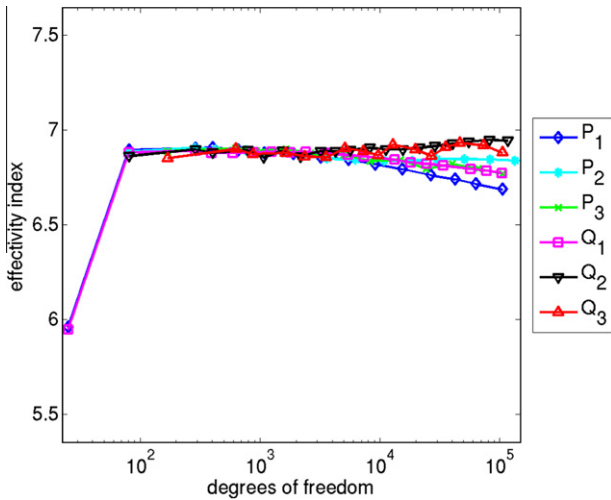


Fig. 5. Example 2. Behavior of the effectivity index of estimator (73) on adaptively refined grids obtained with (72), different finite elements.

Results on adaptively refined quadrilateral grids with hanging nodes will be presented for this example. The initial grid is depicted in Fig. 10. It was refined uniformly until the first grid with more than 2500 degrees of freedom was obtained. Starting from

this grid, an adaptive grid refinement was applied. The simulations were terminated after having computed the first solution with more than 250,000 degrees of freedom. For choosing the mesh cells for refinement, the strategy described at the beginning of this section was applied. Note that for this example $\mu_0 = 0$ and the weights of the estimators (38) are the weights of the estimator (41) times ε . Since the selection procedure for refining the mesh cells is based on a relative comparison of the local error estimates, both estimators lead to the same locally refined grids.

The final adaptively refined grids obtained with the (local counterparts of the) error estimators (38)–(40), and with the error estimator (72) are presented in Fig. 11. It can be seen that the grids look quite differently, in particular for the Q_2 finite element. Whereas the adaptive grid obtained with the L^2 error estimator (39) refines the interior layer completely, the other estimators concentrate the refinement to the neighborhood of the circle. This behavior was already explained in [16]. All estimators start to refine the regions with the strongest layer, which is for the Hemker problem the boundary layer at the circle, in particular in a neighborhood of the point $(-1, 0)$. In this layer, the largest local residuals occur. All error estimators multiply the local residuals by a weight that depends on the size of the mesh cell. The smaller the weights are, the sooner the refinement of large mesh cells in weaker layers will start. Having a look at the weights in (38)–(40) and (72), then it becomes clear that the L^2 estimator (39) will first refine the interior layers, then the H^1 estimator (38) and the robust

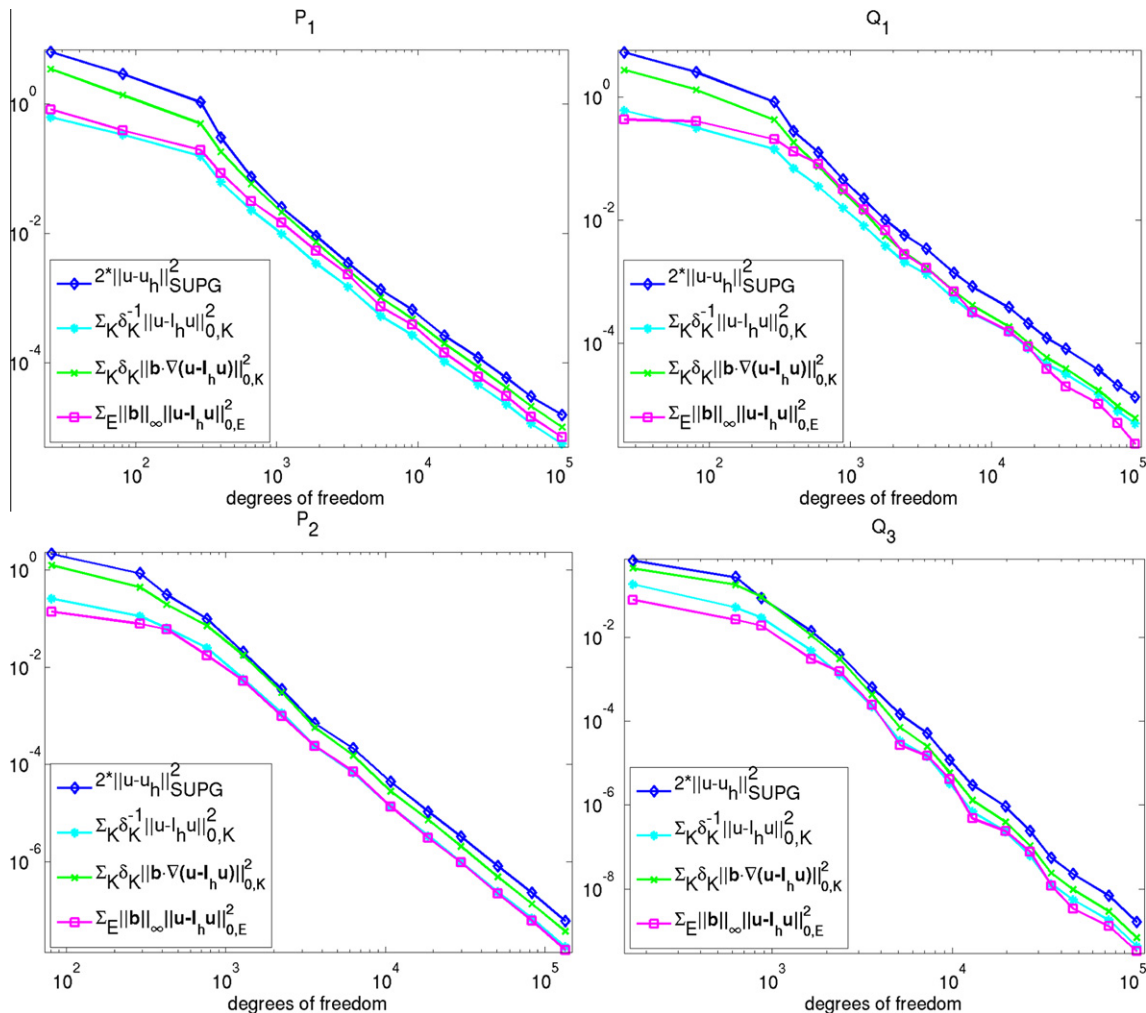


Fig. 6. Example 2. Quantities from hypotheses (14)–(16) with $I_h u$ being the Lagrange interpolant.

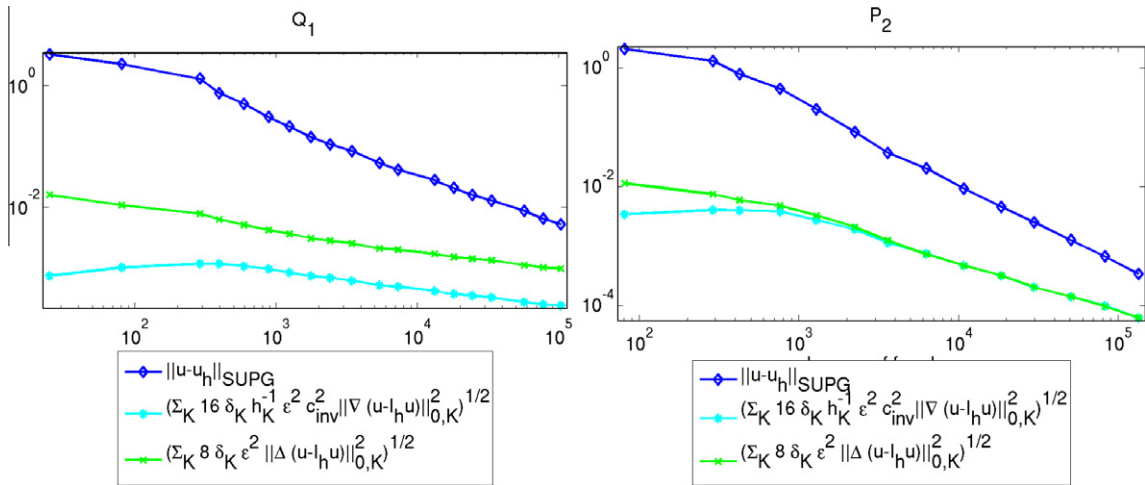


Fig. 7. Example 2. Size of the additional terms on the right hand side of estimate (35) vs. the left hand side.

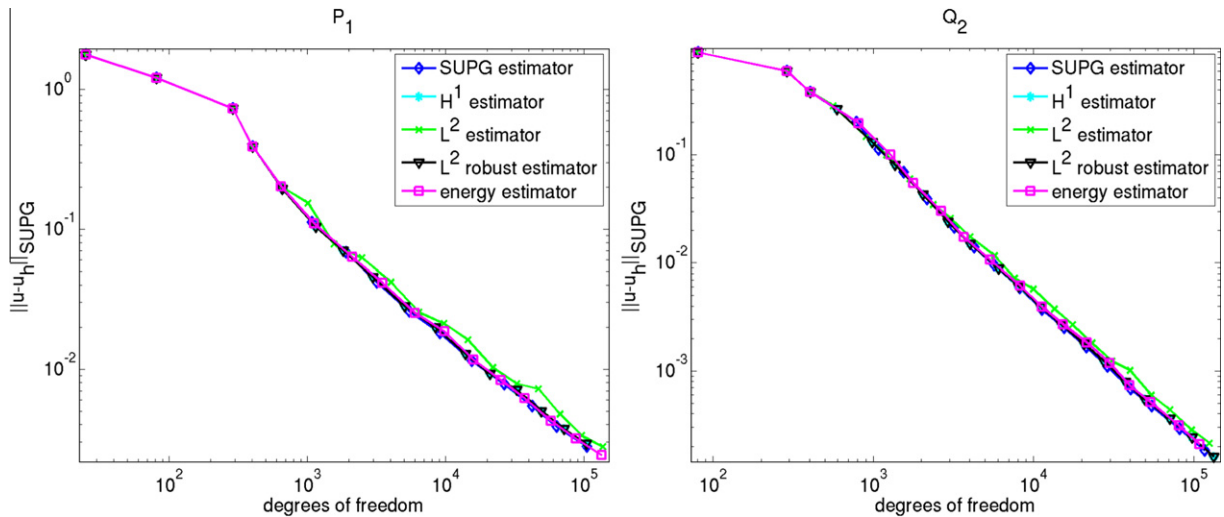


Fig. 8. Example 2. Error in the SUPG norm on adaptively refined grids with different error estimators.

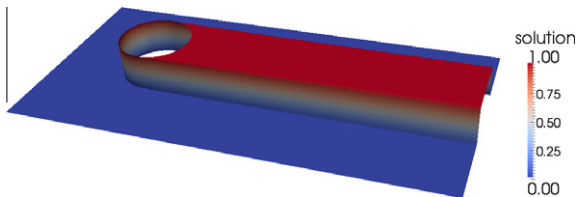


Fig. 9. Solution of the Hemker problem.

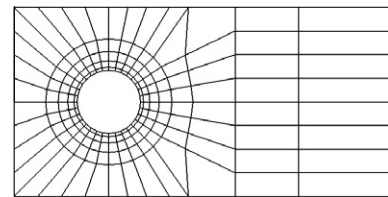


Fig. 10. Hemker problem, initial grid.

$L^2(\Omega)$ estimator (40) will be second, and the SUPG estimator (72) will be last. In this sense, the L^2 estimator refines most uniformly among the considered estimators. This situation can be clearly observed in Fig. 11.

One criterion defined in [2] for the quality of the computed solution is the size of the undershoots and overshoots. It was observed in [2] that for the SUPG solution on uniformly refined grids in particular the size of the undershoots is comparatively large. The largest undershoots occur at the starting points of the interior boundary layers at the circle. Fig. 12 shows that the local grid refinement at the circle leads to a reduction of the undershoots, without removing them. The largest reductions were obtained on the grids computed with the L^2 estimator (39). This statement is also true with respect to the overshoots. Thus, the

better resolution of the region of the interior layers on the grids obtained with the L^2 estimator is also of advantage for the reduction of the spurious oscillations.

Another criterion for the quality of the computed solution defined in [2] is the smearing of the interior layer at $x = 4$, see [2] for a precise definition of the layer width and the reference value. Results with respect to this criterion are presented in Fig. 13. Not surprisingly, the sharpest layers are obtained on the grids computed with the L^2 estimator (39) since these grids are finest in the considered region.

Since a clear conclusion can be already drawn and for the sake of brevity, results concerning the other quality criteria from [2] will be omitted. Having problems with quantities of interest in different kinds of layers, the adaptive grid refinement should be

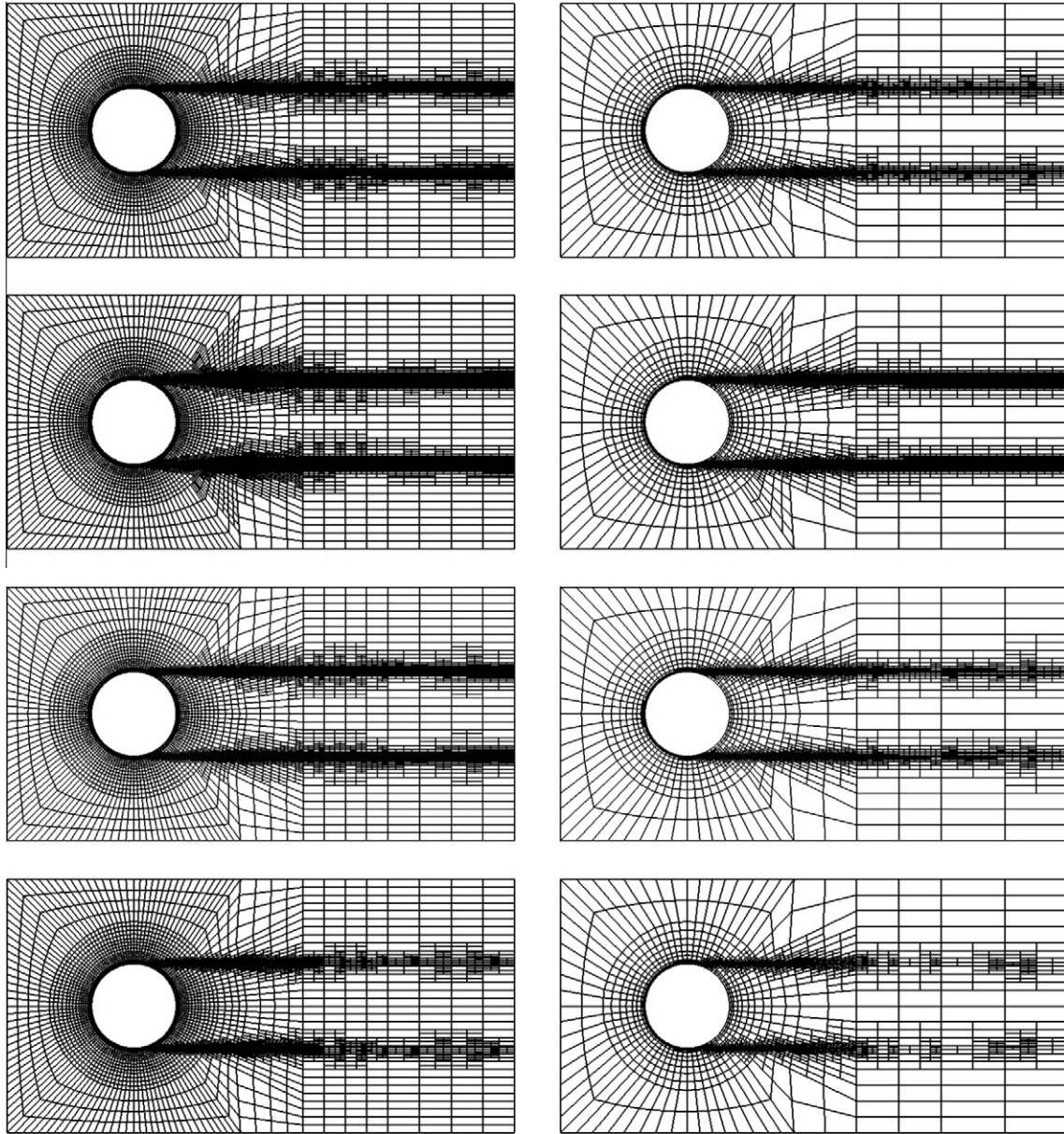


Fig. 11. Hemker problem, final adaptively refined grids, left: Q_1 finite element, right: Q_2 finite element, top to bottom: error estimators (38)–(40) and (72), note that error estimator (41) leads to the same grids as error estimator (38).

controlled by an error estimator that relatively soon selects large mesh cells in weaker layers for refinement. Among the considered error estimators, the L^2 estimator (39) meets this criterion. The use of this estimator for controlling the adaptive grid refinement in this situation was already recommended in [16].

Example 4 (*Example with non-smooth solution*). The derivation of the global upper bound assumed for the solution of (4) that $u \in H^2(\Omega)$, see Lemma 1. Here, the behavior of the proposed error estimator is studied for an example where this assumption is violated. It is defined by $\Omega = (0, 1)^2 \setminus [1/3, 1/3]^2$, $\varepsilon = 10^{-3}$, $\mathbf{b} = (1, 0)^2$, and $c = f = 0$. Homogeneous Dirichlet boundary conditions were described at $x = 0$, $y = 0$, $y = 1$, and homogeneous Neumann boundary conditions at $x = 1$. At the boundary of the interior body, $u = 1$ was prescribed. With this setting, one can expect singularities at the re-entrant corners $(1/3, 1/3)$ and $(1/3, 2/3)$.

Simulations were performed with the P_1 and the Q_1 finite element on uniformly refined grids, see Fig. 14 for the coarsest grids. To approximate the errors, reference solutions were computed on level 10 (more than 33 million of degrees of freedom). Because of the slow convergence due to the singularities, we used for computing the reference solutions the finest grid that was feasible with our hardware. The methodology for performing the numerical studies was as follows. First of all, a value of ε was searched that allows a reliable computation of the errors. To this end, the error in the SUPG norm of the solution on level 1 was computed with the solutions on level 9 and level 10 as reference, respectively. The numerical quadrature was performed on the finer grid. A quadrature rule that is exact for polynomials of degree 19 was used on triangles and a Gaussian quadrature rule that is exact for polynomials of degree 17 on squares. The reference solution on level 10 was considered to be sufficiently accurate if both errors were not much different. This was the case for $\varepsilon = 10^{-3}$ ($\approx 0.3\%$ relative difference) but not for

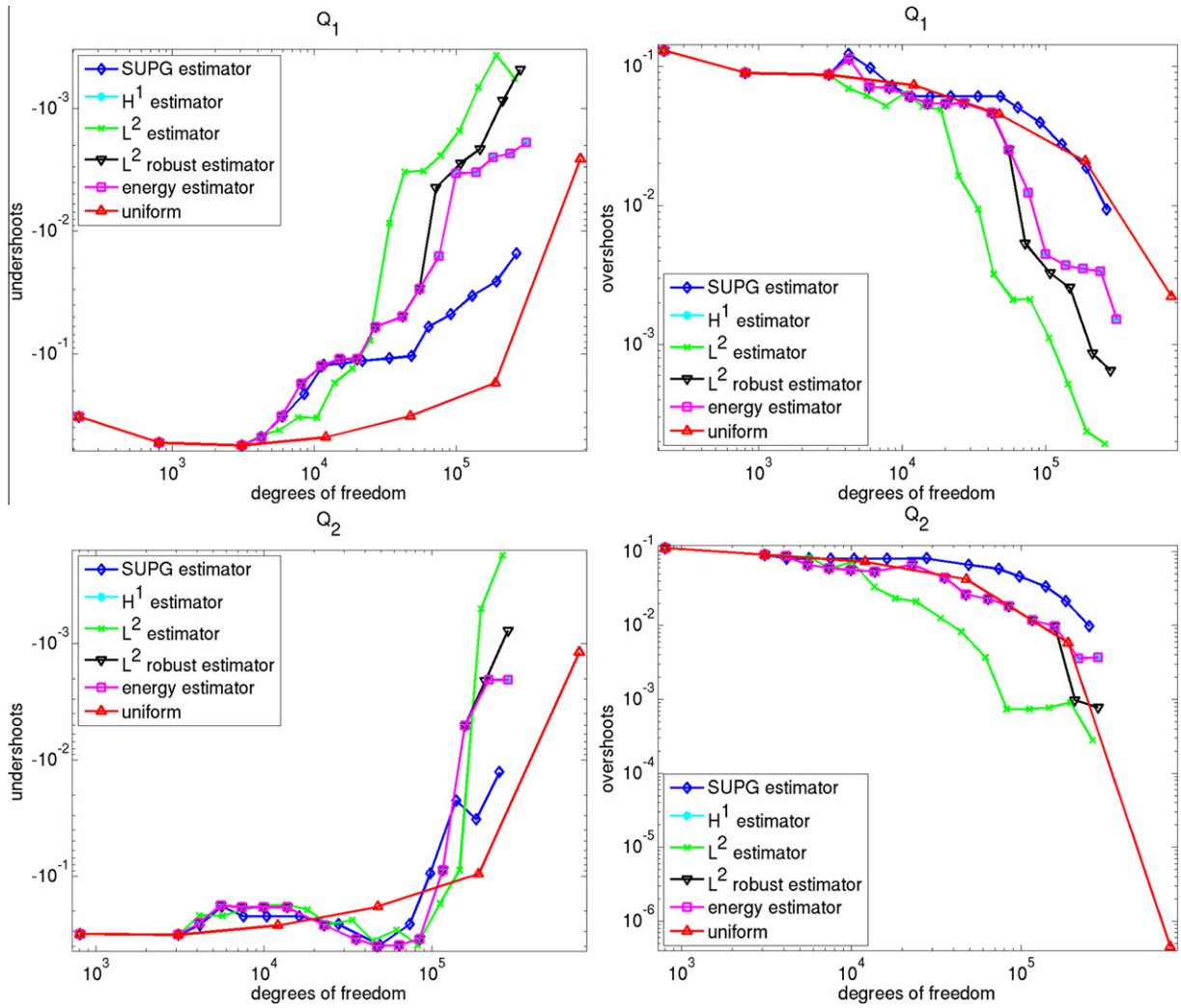


Fig. 12. Hemker problem, undershoots and overshoots.

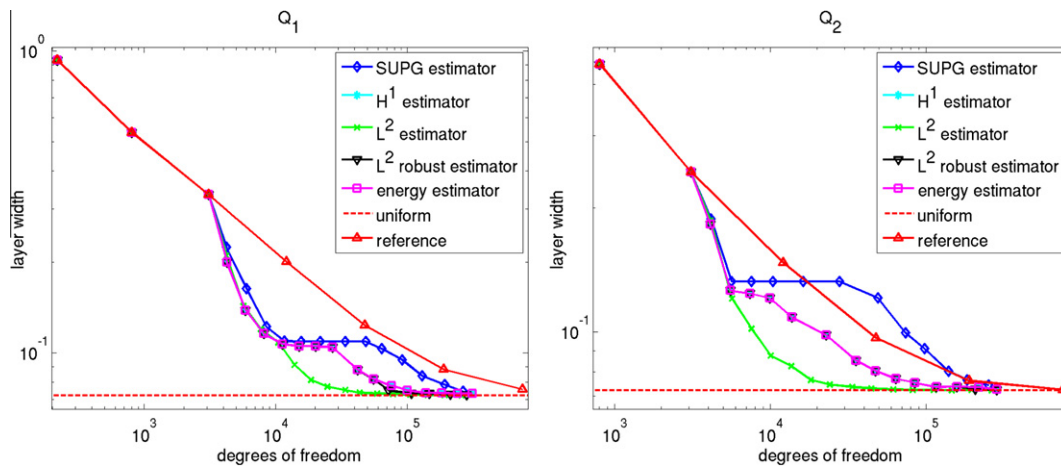


Fig. 13. Hemker problem, layer width at $x = 4$.

$\varepsilon = 10^{-4}$ ($\approx 17\%$ relative difference). Then, all errors for computing the effectivity indices were computed on level 10, after having prolonged the solutions from the coarser grids. Note that the reverse approach, the restriction of the reference

solution to the coarser grids and performing the numerical quadrature on the coarser grids, leads to very inaccurate results since the values and derivatives in the quadrature points on the coarse grids are not taken from the reference solution but only

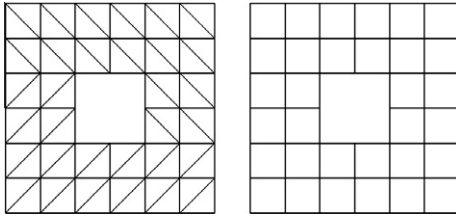


Fig. 14. Example 4. Coarsest grids (level 0).

from its restriction. Since a lot of details of the reference solution are lost by the restriction, the values and derivatives of these two functions might be quite different, in particular in a vicinity of layers.

The SUPG norm is a mesh-dependent norm because it includes the stabilization parameters. Thus, one has to take care to use the mesh-dependent weights from the coarser grids even if the numerical quadrature is performed on the finest grid. The only efficient way to pay attention to this aspect is the use of triangulations where all mesh cells on a given level have the same stabilization parameter. For this reason, uniform grids were considered.

The effectivity indices and results concerning hypotheses (14)–(16) are presented in Fig. 15. From the setup of the numerical simulations, it follows that higher Péclet numbers appear only on the coarsest levels. On the finer levels, already a transition to the diffusion-dominated case starts. All effectivity indices are in the interval [1,8], but there is some increase on finer levels. We observed that the computed errors were usually too small if the level of the reference solution was not sufficiently fine compared with the level of interest. Consequently, the computed effectivity indices were too large in this case. For instance, considering the Q_1 finite element, the solution on level 3 with the reference solution on level 5 gives an effectivity index of 3.85. To obtain an accurate result for level 3 (effectivity index below 2.35), at least the reference solution on level 7 has to be used. Similarly, the effectivity index on level 8 is 8.35 if it is computed with the reference solution from level 9 and it becomes 7.43 for the reference solution computed on level 10, see Fig. 15 for the latter result. Thus, on the one hand, the effectivity indices presented in Fig. 15 might be still somewhat inaccurate (too large) for finer levels. But on the other hand, the diffusion-dominated regime will

be reached soon with further refinement. Then, the effectivity index will be bounded because the estimator is robust in this regime, cf. Remark 4.

To compute the approximations of the left hand sides of (14)–(16), u was taken to be the reference solution and $I_h u$ was computed by first restricting the reference solution to the coarser grids, by taking the values in the corresponding nodes like in the Lagrangian interpolation, and then prolongating this restriction, by inclusion, again to the finest grid. The numerical quadrature was performed on the finest grid, where for computing the left hand side of (16) of course only those edges were used that were present on the respective coarse grid. The results in Fig. 15 show that the approximations obtained in this way fulfill the hypotheses (14)–(16). One can see that the interpolation quantities with stabilization parameters behave differently in the convection- and diffusion-dominated regime.

6. Summary

A residual-based a posteriori error estimator for the SUPG approximation of the solution of convection-dominated convection–diffusion–reaction equations was proposed. The error in the natural SUPG norm is estimated robustly if certain hypotheses are fulfilled that connect the interpolation error in different norms and the error in the SUPG norm. It was discussed that these hypotheses are justified in some standard situation and this statement was supported by numerical results. A numerical analysis without hypotheses and extra terms of the form as in (35) and with weaker assumptions on the regularity of the solution is an open question.

The proposed error estimator possesses different weights than other residual-based estimators for convection–diffusion–reaction equations. These weights cause a deep refinement of the subregion with the strongest singularity before a refinement of subregions with weaker singularities starts. Thus, the proposed estimator can be used for the adaptive grid refinement if the solution possesses only one kind of singularity. It was demonstrated that otherwise the residual-based error estimator (39) for the $L^2(\Omega)$ error should be preferred. But independently of the used error estimator for constructing the adaptive grid, one can expect to obtain with the proposed error estimator a robust estimate of the error in the SUPG norm in the standard situation described in Remark 1.

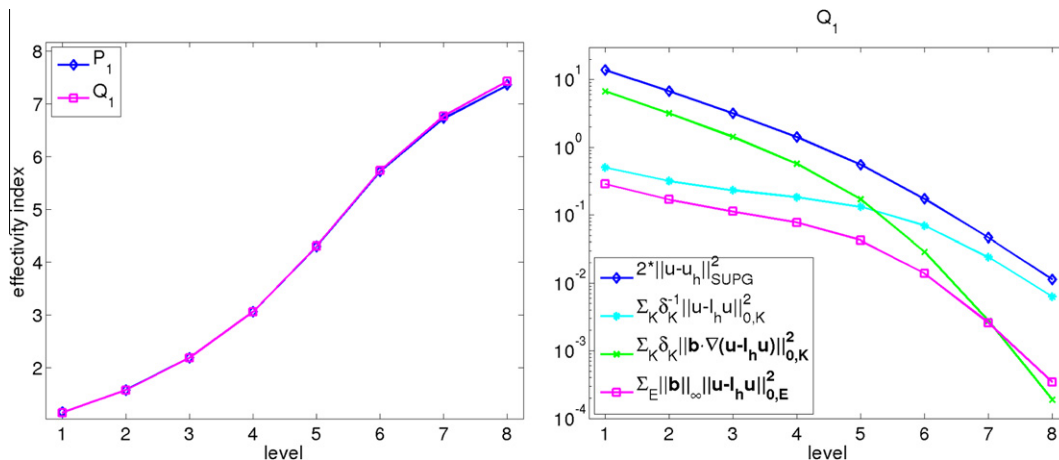


Fig. 15. Example 4. Effectivity indices (left) and quantities from the hypotheses (14)–(16) for the Q_1 finite element (right).

Acknowledgments

We would like to acknowledge three anonymous referees whose suggestions helped us to improve this paper.

References

- [1] Mark Ainsworth, J. Tinsley Oden, A posteriori error estimation in finite element analysis, Pure and Applied Mathematics (New York), Wiley-Interscience [John Wiley & Sons], New York, 2000.
- [2] Matthias Augustin, Alfonso Caiazzo, André Fiebach, Jürgen Fuhrmann, Volker John, Alexander Linke, Rudolf Umla, An assessment of discretizations for convection-dominated convection–diffusion equations, *Comput. Methods Appl. Mech. Engrg.* 200 (47–48) (2011) 3395–3409.
- [3] Alexander N. Brooks, Thomas J.R. Hughes, Streamline upwind/Petrov–Galerkin formulations for convection dominated flows with particular emphasis on the incompressible Navier–Stokes equations, *Comput. Methods Appl. Mech. Engrg.* 32 (1–3) (1982) 199–259 (FENOMECH '81, Part I (Stuttgart, 1981)).
- [4] Erik Burman, A posteriori error estimation for interior penalty finite element approximations of the advection–reaction equation, *SIAM J. Numer. Anal.* 47 (5) (2009) 3584–3607.
- [5] Philippe G. Ciarlet, The finite element method for elliptic problems, *Studies in Mathematics and its Applications*, vol. 4, North-Holland Publishing Co., Amsterdam, 1978.
- [6] Timothy A. Davis, Algorithm 832: UMFPACK V4.3—an unsymmetric-pattern multifrontal method, *ACM Trans. Math. Softw.* 30 (2) (2004) 196–199.
- [7] Isaac Harari, Thomas J.R. Hughes, What are C and h ? : inequalities for the analysis and design of finite element methods, *Comput. Methods Appl. Mech. Engrg.* 97 (2) (1992) 157–192.
- [8] Guillermo Hauke, Mohamed H. Doweidar, Daniel Fuster, A posteriori error estimation for computational fluid dynamics: the variational multiscale approach, *Multiscale Methods in Computational Mechanics*, Lecture Notes in Applied and Computational Mechanics, vol. 55, Springer, Dordrecht, 2011. pp. 19–38.
- [9] Guillermo Hauke, Mohamed H. Doweidar, Daniel Fuster, Antonio Gómez, Javier Sayas, Application of variational a-posteriori multiscale error estimation to higher-order elements, *Comput. Mech.* 38 (4–5) (2006) 356–389.
- [10] Guillermo Hauke, Daniel Fuster, Mohamed H. Doweidar, Variational multiscale a-posteriori error estimation for multi-dimensional transport problems, *Comput. Methods Appl. Mech. Engrg.* 197 (33–40) (2008) 2701–2718.
- [11] P.W. Hemker, A singularly perturbed model problem for numerical computation, *J. Comput. Appl. Math.* 76 (1–2) (1996) 277–285.
- [12] T.J.R. Hughes, A. Brooks, A multidimensional upwind scheme with no crosswind diffusion, *Finite element methods for convection dominated flows*, AMD, vol. 34, American Society of Mechanical Engineers (ASME), New York, 1979 (Papers, Winter Ann. Meeting Amer. Soc. Mech. Engrs., New York, 1979, pp. 19–35).
- [13] T.J.R. Hughes, G. Sangalli, Variational multiscale analysis: the fine-scale Green's function projection optimization localization and stabilized methods, *SIAM J. Numer. Anal.* 45 (2) (2007) 539–557.
- [14] Thomas J.R. Hughes, Multiscale phenomena: Green's functions the Dirichlet-to-Neumann formulation subgrid scale models bubbles and the origins of stabilized methods, *Comput. Methods Appl. Mech. Engrg.* 127 (1–4) (1995) 387–401.
- [15] V. John, J.M. Maubach, L. Tobiska, Nonconforming streamline-diffusion-finite-element-methods for convection–diffusion problems, *Numer. Math.* 78 (2) (1997) 165–188.
- [16] Volker John, A numerical study of a posteriori error estimators for convection–diffusion equations, *Comput. Methods Appl. Mech. Engrg.* 190 (5–7) (2000) 757–781.
- [17] Volker John, Petr Knobloch, On spurious oscillations at layers diminishing (SOLD) methods for convection–diffusion equations. I. A review, *Comput. Methods Appl. Mech. Engrg.* 196 (17–20) (2007) 2197–2215.
- [18] Volker John, Petr Knobloch, Simona B. Savescu, A posteriori optimization of parameters in stabilized methods for convection–diffusion problems. Part I, *Comput. Methods Appl. Mech. Engrg.* 200 (41–44) (2011) 2916–2929.
- [19] Volker John, Gunar Matthies, MoonMD—a program package based on mapped finite element methods, *Comput. Vis. Sci.* 6 (2–3) (2004) 163–169.
- [20] Volker John, Julia Novo, Error analysis of the SUPG finite element discretization of evolutionary convection–diffusion–reaction equations, *SIAM J. Numer. Anal.* 49 (3) (2011) 1149–1176.
- [21] Hans-Görg Roos, Martin Stynes, Lutz Tobiska, Robust numerical methods for singularly perturbed differential equations, *Convection-diffusion-reaction and flow problems*, Springer Series in Computational Mathematics, second ed., vol. 24, Springer-Verlag, Berlin, 2008.
- [22] Giancarlo Sangalli, Robust a-posteriori estimator for advection–diffusion–reaction problems, *Math. Comput.* 77 (261) (2008) 41–70 (electronic).
- [23] Martin Stynes, Steady-state convection–diffusion problems, *Acta Numer.* 14 (2005) 445–508.
- [24] R. Verfürth, A posteriori error estimation and adaptive mesh-refinement techniques, *J. Comput. Appl. Math.* 50 (1–3) (1994) 67–83.
- [25] R. Verfürth, A posteriori error estimators for convection–diffusion equations, *Numer. Math.* 80 (4) (1998) 641–663.
- [26] R. Verfürth, Robust a posteriori error estimates for stationary convection–diffusion equations, *SIAM J. Numer. Anal.* 43 (4) (2005) 1766–1782 (electronic).